QUANTITATIVE ANALYSIS OF APPROXIMATE MODELS TO THE SAINT VENANT EQUATIONS

By

GEORGE PARKER-LAMPTEY, B.Sc.

THESIS

Presented to the Department of Mathematics,

Kwame Nkrumah University of Science and Technology

in Partial Fulfillment of the Requirements for the Degree of

MASTER OF PHILOSOPHY

College of Science

JUNE 2012

Declaration

I hereby declare that this submission is my own work towards the Master of Philosophy (M.Phil.) and that, to the best of my knowledge, it contains no material previously published by another person nor material which has been accepted for the award of any other degree of the University, except where due acknowledgement has been made in the text.

George Parker-Lamptey(PG5072510)	.....	.....
Student	Signature	Date

Certified by:

Prof. S. N. Odai	.....	.....
Supervisor	Signature	Date
Prof. I. K. Dontwi	.....	.....
Supervisor	Signature	Date
Mr. K. K. Darkwah	.....	.....
Head of Department	Signature	Date

Dedication

to my mother, grandmother and two siblings

Naa Odeibaa II, Ayaba Sarpei Cofie, Naa Lamiley and Naa Lamiorkor

with love

Also to the special individuals who have been a blessing to me

Auntie Tsotsoo, Auntie Efua, Naa Koshie, Attoh Dedei, Attoh Korkoi, Yaa Asantewaa,

Naa Adumoyoobi, Whelma and Nana Ama,

Acknowledgements

I am most grateful to Jesus, my Lord and Saviour for his mercies and guidance throughout graduate school and for His Grace by which I can still hope.

I am extremely grateful to my two supervisors, Prof. I. K. Dontwi and Prof. S. N. Odai who have both trained and supported me not only academically but also financially and spiritually. I cannot repay in any form what these men have invested in me.

To Dr. Peter Amoako-Yirenkyi, Mr. K. Darkwa, Mr. J. A. Ackora-Prah and all the lectures in the Department of Mathematics, I thank you for your encouragement and support. God bless you.

Abstract

Approximate models such as (nonlinear Burgers' Equation Model and nonlinear Kinematic Wave Model) to the normalized Saint Venant Equations are very important models that can be used in place of the Saint Venant Equations. In addition to these approximate models, a third order approximate model is proposed and presented in this research. The constants of the previous models are preserved in the third order approximate model and the magnitude of the estimated constant of the third derivative is $F_o^2/3(1-4/9F_o^2)$. The four point Preissmann is used to discretize the normalized Saint Venant Equations and the three approximate models (including the third order model). The algorithms are programmed and the models are simulated. The positive and negative surges are both experimentally considered in the application of a dam break problem. The quantitative results of the approximate models are compared to the normalized Saint Venant equations. The third order derivative is found to equal the Saint Venant equation at lower level than the BEM

Table of Contents

List of Tables

List of Figures

Chapter 1

Introduction

The concept of open channel routing has been thoroughly investigated over time. This chapter focuses on the review of background and research works carried in the area of open channel routing that supports the presented thesis. It has sections that discuss the background studies, problem definition, the objectives within the thesis, the general methodology employed, justification of the problem and the general structure of the thesis.

1.1 Background Studies

The application of *Computational Fluid Dynamics* (CFD) in industrial settings currently span the disciplines of aerospace, automotive, power generation, chemical manufacturing, polymer processing, petroleum exploration, medical research, astrophysics, etc. CFD is the science of predicting fluid flow, heat transfer, mass transfer, chemical reactions, and related phenomena by solving the mathematical equations which govern these processes using a numerical process (discretization methods, solvers, numerical parameters, and grid generations, etc.). The employment of CFD as a tool in these industries has led to reductions in the cost of product, process development and optimization activities. It has also

reduced the need for physical experimentation thereby heightening the overall economic benefit from its usage.

The CFD process begins with a mathematical modeling of a physical problem within which the exact geometry of the problem is defined. The concept of conservation of matter, momentum and energy are incorporated into the model by making sure that the model works within these concepts. The next step is to model the fluid properties empirically and apply simplifying assumptions in order to make the problem tractable (i.e. steady-state, incompressible, inviscid, one-dimensional, etc.) Provision is then made for appropriate initial and boundary conditions for the problem. To be able to solve the problem, the CFD process now uses numerical methods (generally referred to as discretization) to develop approximations of the governing equation of fluid mechanics in the fluid region of interest. The solution arrived at is further post-processed to extract other quantities of interest.

Specific applications of CFD include simulating flow and heat transfer in industrial processes (boilers, heat exchangers, combustion equipment, pumps, pipings, etc.), application in the aerodynamics of ground vehicles, aircraft, missiles, etc. It is also applied in film coating, thermoforming in material processing applications, heat transfer for electronics packaging and so many more. CFD is recognized as an engineering method that provides data that is complementary to theoretical and experimental data. For purely scientific studies, CFD is a useful tool especially in academic institutions and governmental research laboratories.

One particular area that comes under the umbrella of CFD is the study of *hydraulics*;

an applied science and engineering dealing with the mechanical properties of liquids. The branch under hydraulics which deals with free surface flows, occurring in rivers, canals, lakes, estuaries, and seas is referred to as *free surface hydraulics*. The application of studies in this chapter of hydraulics include simulating dam break failures, flood alleviation schemes, sediment transport and river applications. Open channel flow, a further sub-field of free surface hydraulics is the subject of discussion in this thesis. It is simply a field that is centered on describing flow in open channels.

Physical problems in the area of free surface hydraulics and CFD as a matter of fact are governed by well defined set of physical principles which are translated into mathematical statements mostly *partial differential equations*. These statements take the form of equations in which the condition of the particular physical system considered plays the role of the unknown. Scientists and particularly mathematicians make use of mathematical models to describe the behavior of an associated physical system as it responds to a given set of inputs.

An example of models in open channel flow is the Saint-Venant Equations for *channel routing*. Also known as the *shallow water equations*, it is a set of hyperbolic partial differential equations that describe the flow below a pressure surface in a fluid. The fundamental basis of almost all CFD problems are the Navier-Stokes equations, which define any single-phase fluid flow. The Saint-Venant equations are no exception. Particularly important is the use of *non-linear approximate models* to the Saint-Venant Equations for overland flow and channel routing applications; highly motivating are these approximate models in use

because of their simplicity of application with fewer parameters and relatively presentable ease of solutions. Examples of approximate models are the nonlinear Burgers' Equation Model (BEM), Kinematic Wave Model, Modified Puls, Muskingum, Muskingum-Cunge, etc.

With the availability of high speed digital computers which did not happen until the 1960's, problems which were seem impossible to analyze with respect to the nature of solution are now being modeled and solved via numerical methods . The fact is that most hydraulic models in particular the Saint-Venant equations and its approximate models cannot be solved explicitly except by making so many assumptions which are unrealistic for most applications. Numerical techniques are therefore employed in solving these equations. Three groups of methods are usually used : finite difference, finite element and finite volume (Sleigh and Goodwill (2000)). These result in computer programs that help to simulate the problem at hand. For flow problems, the simulation involves flow variables such as discharge, velocity, depth cross-section, volume and duration (time). The propagation of particular interest are peak, time it takes to peak, duration of the hydrograph and attenuation. Applications of channel routing models especially in the management of water resources (Su Ki Ooi (2005)) has created a high demand for computer programs which simulate routing variables peculiarly variables based on the one-dimensional Saint-Venant Equations. Examples of solvers (computer programs) are MIKE - computer program that includes full solution of the Saint-Venant equations, XPSWM - computer software package for dynamic modeling of storm water, HEC-RAS - computer program that models

hydraulics of water flow (unsteady), MIKE FLOOD, two dimensional MIKE 21, DIVAST, LISFLOOD-FP, SOBEK, 1D2D, etc.

Approximate models and their dominance is not a new concept especially in an area like hydraulics with reference to computer programs. The need for approximate models is deeply rooted in the fact that the 'parent' models are very complex and need comparatively more parameters to run or simulate.

In hydraulics, there are two main branches of approximate models for simulating translatory waves in waves in conveyance. These are the diffusive and the kinematic models. The wide applications of these approximate models are because they are simple and provide solutions with ease. Price (1994) stated that the nonlinear approximate models serve as better teaching tools for understanding nonlinear phenomena and have value of rapid calculations.

Tsai (2003) also discussed the fact that the simplified routing models have fewer parameters and tend to have advantages in terms of feasibility and practicality when used for real-time flood operations. An additional advantage is that simplified models need significantly less computational requirement in terms of time and data (Singh et al 1998).

The simplest of all existing approximate models is the Kinematic Wave Model (Lighthill and Whitham) although it cannot account for downstream influences such as tides on the translatory wave [see —Price (1994), Onizuka and Odai (1998), S. N. Odai (1999)].

S. N. Odai (1999) developed an approximate model, the nonlinear Kinematic Wave Model for predicting open channel flow rate. This was based on the full Saint Venant equa-

tions and assumed two constants estimated and expressed in terms of the froude number of initial flow. The Kinematic Wave Model gave close results to the Saint Venant equations under subcritical flow and for a given flow depth at the upstream end of the channel, the approximate magnitude of flow rates at the downstream section is readily obtained in analytical form. Other advantages of the KWM was in its simplicity and ease of application; requiring less computation time comparatively to the SVE.

Literature documents the diffusive type of models as better compared to the Kinematic Wave Models [see Akan and Yen (1977), Price (1994)] with which some reliable results have been developed. They however do not place any significant advantage compared to the SVE because the diffusive models cannot be solved analytically except for the reduction in simulation time for numerical solution. The Burgers' Equation, a form of nonlinear diffusion equation is the simplest integrable mathematical formulation that shows the interplay between nonlinear and diffusion effects on a propagatory wave [Burgers (1950), Whitham (1974)].

The Burgers' Equation Model that approximated the full SVE assuming that flow velocity depends on flow depth and its gradient was presented by Onizuka and Odai (1998) as a single lower-ordered equation that approximately described unsteady flow in a wide rectangular open channel. The research was based on the normalized system of the Saint Venant equations by Kubo and Shimura (1999).

K. Odai Onizuka and Osato (2006) presented an analytical solution of Burgers' equation for simulating translatory waves in conveyance channels. In this research, K. Odai

Onizuka and Osato (2006) upgraded the previous Burgers' equation model (Onizuka and Odai (1998)) for small perturbations in initial uniform flow approximated using the SVE. The analytical solution of the presented Burgers' equation was done using Cole-Hopf and solved via Green's function and this was compared to the Saint Venant equations solved numerically by cubic-interpolated pseudo-particle scheme (Yabe and Aoki (1991)) . The research findings indicated that the Burgers' Equation Model captures well the characteristics of translatory wave moving in conveyance channels and hence could be useful for simulating flood movement and for predicting the flow rate when the flow at an upstream section is given.

1.2 Problem Definition

The Saint Venant equations are commonly used for prediction and control design for irrigation channels, see Malaterre and Baume (1998) for an overview. Su Ki Ooi (2005) demonstrated that the Saint Venant Equations can adequately capture the dynamics of real channels and even concluded in the research that naturally, the model with estimated parameters is more accurate than the one with physical parameters. Therefore on a qualitative scale, the significance of the dynamic model together with the present two class of approximate models is known. The exact quantum of errors associated with using the approximate models compared with the dynamic model is however unknown.

It is against this background that the researcher would like to investigate the quantitative comparisons of the approximate models and the dynamic model. As presented in

the background studies above, there has been considerable discussion of the qualitative predictions of the dynamic and its approximate models. Also since the BEM and KWM are approximated using second order derivative equation and first order derivative equations respectively, the researcher proposes and presents a third order derivative equation to examine the effect of adding extra derivative terms as a form of approximating the parent model.

1.3 Objectives

In the light of the presentation made, the key objective of this study is to estimate a third order approximate equation to the Saint Venant equation and compare the present approximate models together with the proposed third order approximate equation to the Saint Venant Equations.

- estimate a third order approximate model to the Saint Vennat Equations
- use the implicit Preissmann scheme to discretize and solve the SVE, BEM, KWM and the proposed third order approximate model
- run an error analysis of the approximate models against the dynamic model
- investigate the exact range of the flow depth difference within which these models present acceptable results

1.4 Methodology

This thesis presents both analytical solutions and numerical solutions of the two approximate models and the dynamic models discussed. The analytical solution of the Saint Venant equations is by the method of characteristics. More important, is the use of implicit finite difference methods to present numerical solutions of the considered models. The SVE, BEM, KWM and the proposed model are all solved using the Preissmann scheme. The sparse systems of equations that result from the implicit schemes are solved via standard methods for solving systems of linear algebraic equations. Within the solution for the SVE and the KWM using the Preissmann scheme, we encounter a nonlinear system of equations for which the Newton algorithm for nonlinear systems of equations is used to solve. This reduces to a banded system of linear equations which is taken advantage of Szymkiewicz (2010).

After solution of the models, we use error analyzing techniques to investigate the performance of the models. The numerical algorithms from the finite difference scheme are programmed using MATLAB R2007b. The simulation for the models and error analysis computation is entirely done using MATLAB R2007b.

1.5 Justification of Study

The nonexistence of analytical solutions of the dynamic model and its approximate models without any assumption or simplification makes any research that is aimed at finding

alternate (approximate) solution in relation to the subject very relevant. This thesis will provide algorithms for the normalized Saint Venant Equations based on the four-point implicit Preissmann scheme and for the approximate models. The quantitative comparison also sets the stage for very simple approximate models to be used instead of the dynamic model with knowledge of thier divergence from the actual solution.

1.6 Structure of the Thesis

The structure of the thesis is given as follows.

- Chapter 2 presents an introduction of the Saint-Venant equations. The two approximate models are also derived from the normalized set of the Saint-Venant equations.
- Chapter 3 discusses the methodology employed in our study.
- Chapter 4 presents the analysis from the simulation results.
- Chapter 5 presents the conclusion and recommendations for further research

Chapter 2

Mathematical Models

2.1 Introduction

In this chapter, we present a general overview of the hydraulic models which are of consideration with respect to this thesis. We begin by looking at the shallow water equations by presenting it in a term by term procedure and introduce the Burgers' Equation model (BEM) and the Kinematic Wave Model (KWM). The derivation and general highlights of the proposed third order approximate model is presented here.

2.2 Channel Routing Models

Shallow water equations are the commonly used models under open channel flow. They are placed with the assumption that the flow is shallow relative to the dimensions of the problem under consideration. The basis for the formation is a *continuity equation* which corresponds to conservation of mass and an application of the laws of governing classical physics which is used to generate the *equation of motion*. Depending on their construction, such equations are often written as conservation laws representing the conservation of a

particular quantity such has momentum or energy. Then there is an addition of terms to account for the effects such as friction, geometry variation, viscosity, etc. These additional terms are often referred to as *source terms* which generally correspond to some sort of loss or gain from the system.

In the preceding sections, of this chapter, the Saint-Venant equations are introduced together with its alternate forms. The set of these partial differential equations in however form presented called the Saint-Venant equation are also known as shallow water equations.

An introduction of the two approximate models (Burgers' Equation Model and the Non-linear Kinematic Wave Model) is also presented. Finally attached to these presentations is the derivation of the third order approximate model.

2.3 The Saint Venant Equations

These are the most commonly used set of equations that constitute a system in one-dimensional flows for open channel flow problems. They are used to describe gradually varied flow of an incompressible inviscid fluid. The Saint Venant Equations (SVE) are a set of hyperbolic partial differential equations that describe flow below a pressure surface in a fluid. This model was developed by a mathematician and mechanician named Adhe'mar Jean Claude Barre' de Saint-Venant (August 23,1797, Villiers-en-Biere, Seine-et-Marne-January 1886, Saint-Ouen, Loir-et-Cher). It is a combination of the principles of continuity (conservation of mass) and momentum (essentially Newton's second law of motion). These set of equations are primarily from the Navier Stokes equations.

Mathematically, given that Q is the discharge (m^3/sec), A is the cross-sectional area, q is the lateral flow per unit length of the channel ($m^3/sec/m$), x is the distance along the channel, y is the depth of flow, g is the acceleration due to gravity, S_0, the bed slope of the channel and S_f the friction slope, the governing equations are written as :

$$\begin{aligned} \frac{\partial Q}{\partial x} + \frac{\partial (A)}{\partial t} &= q \qquad \text{(continuity)} \\ \left(\frac{1}{A}\right)\frac{\partial Q}{\partial t} + \left(\frac{1}{A}\right)\frac{\partial \left(Q^2/A\right)}{\partial x} + g\frac{\partial y}{\partial x} - g(S_0 - S_f) &= 0 \qquad \text{(momentum)} \end{aligned}$$

where the defined variables are given as follows

- $1/A(\partial Q/\partial t)$ - local acceleration terms which describes the change in the momentum due to change in velocity over time
- $(1/A)\partial\left(Q^2/A\right)/\partial x$ - connective acceleration term which describes the change in momentum due to change in velocity along the channel
- $g\partial y/\partial x$ - pressure force term representing the force proportional to the change in water depth along the channel

The last two terms is a combination of the gravity force and the friction force terms which describe the force proportional to the bed slope and the friction slope respectively.

The assumptions underlying the Saint-Venant Equations are :

- the bed slope is small resulting in the cosine of the angle between the bed level and the horizontal begin approximately one.

- the pressure is hydrostatic (that is the streamline curvature is small and the vertical accelerations are negligible).

- the effects of the boundary friction and turbulence can be accounted for by representations of channel conveyance derived from steady-state flow

The momentum equation presented is expressed in conservative form. It is possible to substitute uA for Q in the continuity equation and the momentum equation. An expansion of the momentum equation and a further simplification using the continuity equation produces a mathematically correct *non-convective form* of the momentum equation. Use of the non-convective form may however lead to practical difficulties in its numerical solution. (Nelz and Pender (2009)).

Alternate forms of the Saint Venant equations include:

1. Using Q and h

$$\begin{aligned} \frac{\partial h}{\partial t} + \frac{1}{B}\frac{\partial Q}{\partial x} &= 0 \\ \frac{\partial Q}{\partial t} + \frac{\partial}{\partial x}\left(\frac{Q}{A}\right) + gA\frac{\partial h}{\partial x} + gA(S_f - S_0) &= 0 \end{aligned}$$

2. Using Q and y where y is the surface elevation of the platform

$$\begin{aligned} \frac{\partial y}{\partial t} + \frac{1}{B}\frac{\partial Q}{\partial x} &= 0 \\ \frac{\partial Q}{\partial t} + \frac{\partial}{\partial x}\left(\frac{Q}{A}\right) + gA\frac{\partial y}{\partial x} + gAS_f &= 0 \end{aligned}$$

3. Using u and h

$$\begin{aligned} \frac{\partial h}{\partial t} + \frac{A}{B}\frac{\partial u}{\partial x} + u\frac{\partial h}{\partial x}\frac{u}{B}\left(\frac{\partial A}{\partial x}\right)_{h=const} &= 0 \\ \frac{\partial u}{\partial t} + u\frac{\partial u}{\partial x} + g\frac{\partial h}{\partial x} + g(S_f - S_0) &= 0 \end{aligned}$$

4. Using u and y

$$\begin{aligned} \frac{\partial u}{\partial t} + \frac{A}{B}\frac{\partial u}{\partial x} + u\left(\frac{\partial y}{\partial x} + S_0\right) + \frac{u}{B}\left(\frac{\partial A}{\partial x}\right)_{y=const} &= 0 \\ \frac{\partial u}{\partial t} + u\frac{\partial u}{\partial x} + g\frac{\partial y}{\partial x} + gS_f &= 0 \end{aligned}$$

Another important alternate form of the Saint-Venant equations considered for wide rectangular open channels is given by

$$\frac{\partial h}{\partial t} + \frac{\partial (uh)}{\partial x} = 0 \qquad \text{(continuity equation)} \qquad (2.1)$$

$$\frac{\partial u}{\partial t} + u\frac{\partial u}{\partial x} + \frac{\partial h}{\partial x} + \frac{1}{F_o^2}\frac{u^2}{h^{2m}} - 1 = 0 \qquad \text{(dynamic equation)} \qquad (2.2)$$

where h = flow depth; u = flow velocity; x = distance in flow direction; t = time; g = acceleration due to gravity; S_0 = channel bottom slope and S_f = friction slope.

Considering H = initial normal depth; L = reference channel length ($= H/S_0$); U = celerity of a shallow wave ($= \sqrt{gH}$) and T = time constant ($= L/\sqrt{gH}$).

Then the flow variables can be normalized with the normalized variables given as follows:

$$h' = \frac{h}{H} \;\; x' = \frac{x}{L} \;\; u' = \frac{u}{U} \;\; t' = \frac{t}{T}$$

With these conversions and replacement of the variables themselves by dropping the primes, (2.1) and (2.2) can be converted to a normalized system of Saint Venant equations

by Kubo and Shimura (1999) as

$$\frac{\partial h}{\partial t} + \frac{\partial (uh)}{\partial x} = 0 \tag{2.3}$$

$$\frac{\partial u}{\partial t} + u\frac{\partial u}{\partial x} + \frac{\partial h}{\partial x} = 1 - \frac{1}{F_0^2}\frac{u^2}{h^{2m}} \tag{2.4}$$

with all the primes dropped from the variables. F_0 is the froude number of initial uniform flow and it is given by

$$F_0 = \frac{H^m \sqrt{S_0}}{nU}$$

where n = Manning's roughness coefficient; and $m = 2/3$ for Manning's formular and $m = 1/2$ for Chezy's formular.

Equations (2.3) and (2.4) will be used throughout this thesis as the Saint Venant equations.

2.4 Kinematic Wave Equation

The non-linear Kinematic equation is given by

$$\frac{\partial h}{\partial t} + (\alpha + \beta h)\frac{\partial h}{\partial x} = 0 \tag{2.5}$$

is extracted from the continuity equation (2.3) and a reduced form of the momentum equation (2.4) assuming small perturbations in the initial normal depth. The constants in the equation are given as

$$\alpha = \frac{5}{9}F_o; \quad \beta = \frac{10}{9}F_o \text{ and } \alpha + \beta = \frac{5}{3}F_o \tag{2.6}$$

2.5 The Burgers' Equation Model

The Burgers' equation model is simplest integrable mathematical formulation that shows the complicated interplay between nonlinear and diffusion effects on a wave (see Burgers (1950)). Onizuka and Odai (1998) extracted the Burgers' equation of the form

$$\frac{\partial h}{\partial t} + (\alpha + \beta h)\frac{\partial h}{\partial x} - \upsilon \frac{\partial^2 h}{\partial x^2} = 0 \tag{2.7}$$

from the Saint Venant equations (2.3) and (2.4) assuming small perturbations in the initial normal depth. The constants within the Burgers' equation are given as

$$\alpha = \frac{5}{9}F_o; \quad \beta = \frac{10}{9}F_o; \quad \upsilon = \frac{F_o}{2}\left(1 - \frac{4}{9}F_o^2\right); \quad \alpha + \beta = \frac{5}{3}F_o$$

The model is applicable within the range $0 < F_o < 3/2$ [see Odai et al (2006)]

2.6 The Proposed Third Order Approximate Model

The proposed third order derivative approximate model is given by

$$\frac{\partial h}{\partial t} + (a + bh)\frac{\partial h}{\partial x} - c\frac{\partial^2 h}{\partial x^2} + d\frac{\partial^3 h}{\partial^3 x^3} = 0 \tag{2.8}$$

The following is the derivation of the coefficient constants within the model

2.6.1 Estimation of Model Constants

From continuity and dynamic equations assuming small perturbations in the initial normal depth. Eqn (2.8) satisfies the continuity equation if the flow rate per unit width, uh, satisfies the equation

$$uh = ah + 0.5bh^2 - c\frac{\partial h}{\partial x} + d\frac{\partial^2 h}{\partial x^2} + K \tag{2.9}$$

where K is constant. At the initial uniform flow, where $h = 1$, $u = F_0$ the first and second derivatives of h with respect to x equals zero

$$\begin{aligned} F_0 &= a + 0.5b + K \\ \Rightarrow K &= F_0 - a - 0.5b \end{aligned}$$

The flow velocity, u can then be expresed in terms of the flow depth, h as

$$u = \left(F_0 + a(h-1) + 0.5b(h^2-1) - c\frac{\partial h}{\partial x} + d\frac{\partial^2 h}{\partial x^2} \right) / h \tag{2.10}$$

From Eqn (2.10), we can calculate the following variables

$$\begin{aligned} u^2 = & \frac{\left[F_0 + a(h-1) + 0.5b(h^2-1)\right]^2}{h^2} - \frac{-2c\left[F_0 + a(h-1) + 0.5b(b^2-1)\right]}{h^2}\frac{\partial h}{\partial x} \\ & + 2d\frac{\left[F_0 + a(h-1) + 0.5b(h^2-1)\right]^2}{h^2} - \frac{-2c\left[F_0 + a(h-1) + 0.5b(b^2-1)\right]}{h^2}\frac{\partial^2 h}{\partial x^2} \\ & - \frac{cd}{h^2}\frac{\partial h}{\partial x}\left(\frac{\partial^2 h}{\partial x^2}\right) + \frac{c^2}{h^2}\left(\frac{\partial^2 h}{\partial x^2}\right)^2 + \frac{d^2}{h^2}\left(\frac{\partial^2 h}{\partial x^2}\right)^2 \end{aligned} \tag{2.11}$$

$$\frac{\partial u}{\partial x} = \frac{[F_0 + a + 0.5bh^2 + 0.5b]}{h^2}\frac{\partial h}{\partial x} - \frac{c}{h}\frac{\partial^2 h}{\partial x^2} + \frac{d}{h}\frac{\partial^3 h}{\partial x^3} + \frac{c}{h^2}\left(\frac{\partial h}{\partial x}\right)^2 - \frac{d}{h^2}\left(\frac{\partial h}{\partial x}\right)\left(\frac{\partial^2 h}{\partial x^2}\right) \tag{2.12}$$

$$\begin{aligned} u\frac{\partial u}{\partial x} = & \frac{1}{h^3}[F_0 + a(h-1) + 0.5b(h^2-1)][-F_0 + a + 0.5bh^2 + 0.5b]\frac{\partial h}{\partial x} \\ & - \frac{c}{h^2}[F_0 + a(h-1) + 0.5b(h^2-1)]\frac{\partial^2 h}{\partial x^2} + \frac{d}{h^2}[F_0 + a(h-1) + 0.5b(h^2-1)]\frac{\partial^3 h}{\partial x^3} \\ & + \frac{c}{h^3}[2F_0 - 2a + ah - b]\left(\frac{\partial^2 h}{\partial x^2}\right)^2 + \frac{c^2 + dh(-2F_0 - ah + 2a + b)}{h^2}\left(\frac{\partial h}{\partial x}\right)\left(\frac{\partial^2 h}{\partial x^2}\right) \\ & - \frac{cd}{h^2}\left(\frac{\partial h}{\partial x}\right)\left(\frac{\partial^3 h}{\partial x^3}\right) - \frac{c^2}{h^3}\left(\frac{\partial h}{\partial x}\right)^3 + \frac{cd}{h^3}\left(\frac{\partial h}{\partial x}\right)^2\left(\frac{\partial^2 h}{\partial x^2}\right) - \frac{cd}{h^2}\left(\frac{\partial^2 h}{\partial x^2}\right)^2 \\ & \frac{d^2}{h^2}\left(\frac{\partial^2 h}{\partial x^2}\right)\left(\frac{\partial^3 h}{\partial x^3}\right) + \frac{cd}{h^3}\left(\frac{\partial^2 h}{\partial x^2}\right)^3 - \frac{d^2}{h^3}\left(\frac{\partial h}{\partial x}\right)\left(\frac{\partial^2 h}{\partial x^2}\right)^2 \end{aligned} \tag{2.13}$$

$$\begin{aligned} \frac{\partial u}{\partial t} = & \frac{1}{h}\left[(a + bh)\frac{\partial h}{\partial t} - c\frac{\partial}{\partial x}\left(\frac{\partial h}{\partial t}\right) + d\frac{\partial^2}{\partial x^2}\left(\frac{\partial h}{\partial t}\right)\right] - \\ & \frac{1}{h^2}\frac{\partial h}{\partial t}\left[F_0 + a(h-1) + 0.5b(h^2-1) - c\frac{\partial h}{\partial x} + d\frac{\partial^2 h}{\partial x^2}\right] \end{aligned} \tag{2.14}$$

However from the proposed third order approximate model we are able to find an expression for $\partial h/\partial t$ (2.15) and evaluate the first and second derivatives of $\partial h/\partial t$ with respect to x as shown in equations (2.16) and (2.17).

$$\frac{\partial h}{\partial t} = -(a+bh)\frac{\partial h}{\partial x} + c\frac{\partial^2 h}{\partial x^2} - \frac{\partial^3 h}{\partial x^3} \tag{2.15}$$

$$\frac{\partial}{\partial x}\left(\frac{\partial h}{\partial t}\right) = -b\left(\frac{\partial h}{\partial x}\right)^2 - (a+bh)\frac{\partial^2 h}{\partial x^2} + c\frac{\partial^3 h}{\partial x^3} - d\frac{\partial^4 h}{\partial x^4} \tag{2.16}$$

$$\frac{\partial^2}{\partial x^2}\left(\frac{\partial h}{\partial t}\right) = -2b\frac{\partial^2 h}{\partial x^2} - b\left(\frac{\partial h}{\partial x}\right)\left(\frac{\partial^2 h}{\partial x^2}\right) - (a+bh)\frac{\partial^3 h}{\partial x^3} + c\frac{\partial^4 h}{\partial x^4} - d\frac{\partial^5 h}{\partial x^5} \tag{2.17}$$

Therefore

$$\begin{aligned}\frac{\partial u}{\partial t} = {} & \frac{(a+bh}{h^2}[F_0 - a - 0.5bh^2 - 0.5b]\frac{\partial h}{\partial x} + \frac{c[-F_0 + a(h+1) + 0.5b(3h^2+1)]}{h^2}\left(\frac{\partial^2 h}{\partial x^2}\right) \\ & + \frac{-2h(bd+c^2) + d[F_0 + a(h+1) + 0.5b(h^2-1)]}{h^2}\frac{\partial^3 h}{\partial x^3} + \frac{2cd}{h}\frac{\partial^4 h}{\partial x^4} - \frac{d^2}{h}\frac{\partial^5 h}{\partial x^5} \\ & - \frac{ac}{h^2}\left(\frac{\partial h}{\partial x}\right)^2 + \frac{ad+c^2}{h^2}\left(\frac{\partial h}{\partial x}\right)\left(\frac{\partial^2 h}{\partial x^2}\right) - \frac{cd}{h^2}\left(\frac{\partial h}{\partial x}\right)\left(\frac{\partial^3 h}{\partial x^3}\right) + \frac{d^2}{h^2}\left(\frac{\partial^2 h}{\partial x^2}\right)\left(\frac{\partial^3 h}{\partial x^3}\right) \\ & \frac{cd}{h^2}\left(\frac{\partial^2 h}{\partial x^2}\right)^2\end{aligned} \tag{2.18}$$

Substituting these expressions (2.11), (2.13) and (2.18) into the assumed proposed third order approximate model (2.18), simplifying and averaging terms with the same derivative coefficients results in

$$A(h) = A_0(h) + A_1(h)\frac{\partial h}{\partial x} + A_2(h)\frac{\partial^2 h}{\partial x^2} + A_3(h)\frac{\partial^3 h}{\partial x^3} + \cdots \tag{2.19}$$

where

$$\begin{aligned}A_0(h) = {} & 1 - \frac{\left[F_o + a(h-1) + 0.5b(h^2-1)\right]^2}{F_o^2 h^{2m+2}} \\ A_1(h) = {} & 1 - 2c\frac{\left[F_o + a(h-1) + 0.5\beta(h^2-1)\right]^2}{F_o^2 h^{2m+2}} + \frac{(a+bh)}{h^2}[F_0 - a - 0.5bh^2 - 0.5b] \\ & \frac{1}{h^3}[F_0 + a(h-1) + 0.5b(h^2-1)][-F_0 + a + 0.5bh^2 + 0.5b] \\ A_2(h) = {} & \frac{c[-F_0 + a(h-1) + 0.5b(3h^2+1)]}{h^2} - \frac{c}{h^2}[F_0 + a(h-1) + 0.5b(h^2-1)] + \\ & \frac{2d[F_0 + a(h-1) + 0.5b(h^2-1)}{F_0^2 h^{2m+2}}\end{aligned}$$

A very important note at this point is the fact that since the proposed model is an approximation of the Saint Venant equations, not every term in the expression for $A(h)$ (2.19) can be eliminated.

The normalized Saint Venant equations explicitly specify a relation between the first derivatives of the flow variables. Thus here, the first three derivatives are eliminated for small perturbations of flow depth about the initial constant.

At $h = 1, A_0(h) = 0$. Taking the first derivative of $A_0(h)$ with respect to h at $h = 1$ gives the expression $(a + b)$ [i.e. from $A_0'(1)$]; Then taking the second derivative of $A_0(h)$ with respect to h at $h = 1$ gives an expression for b [i.e. $A_0''(1)$]. c is obtained from $A_1(1)$. The last constant d is obtained from $A_2(h)$ at $h = 1$. Thus the coefficients of the third order approximate model to the Saint Venant Equation are given by

$$a = \frac{5}{9}F_o; \quad b = \frac{10}{9}F_o; \quad c = \frac{F_o}{2}\left(1 - \frac{4}{9}F_o^2\right); \quad a + b = \frac{5}{3}F_o \quad d = -\frac{F_o^2}{3}\left(1 - \frac{4}{9}F_o^2\right)$$

Chapter 3

Methodology

3.1 Numerical Methods

Numerical Methods in its entirety is the transformation of mathematical models into an algebraic, linear or non-linear, system of equations for mesh/grid - related unknown quantities. The transformation procedure is referred to as *discretization* or space discretization where a mesh/grid is set up and the continum of space is replaced by a finite number of points where the numerical of the variable will have to be determined. The accuracy of the numerical results is critically dependent on the mesh quality.

Numerical methods can generally be classified as:

1. Finite Difference Methods (FDM)
2. Finite Element Methods (FEM)
3. Spectral Methods
4. Finite Volume Methods (FVM)

We shall discuss an overview of all the methods and pay particular attention to FDM which we will make use of in this thesis.

In general terms, finite difference methods represent the problem through a series of points or nodes. Expressions for the unknown are derived via replacing the derivative terms in the model equation with truncated or approximate Taylor series expansions. The earliest numerical schemes were based on finite difference schemes and are conceptually and intuitively one of the easier methods amongst the given classification to implement. Most texts describe finite difference as the most traditional and oldest of numerical methods. However, fundamentally such techniques require a high degree of regularity with the mesh and so this limits their application to complex problems.

Finite element method employs the use of dividing the domain into elements such as triangles or quadrilaterals and to place with each element nodes at which the numerical solution is determined. The solution at any position is then represented by a series expansion of the nodal values within the local vicinity of that position. The nodal contributions are multiplied by basis functions (also known as shape, interpolation, or trial functions) and the particular way in which the basis functions are defined determines the choice of variant of the finite element method. Spectral methods can be considered as a subset of the finite element method in which the basis functions are defined globally as opposed to the more common approach whereby the basis functions are local and so one zero outside the neighborhood of the associated node. The original finite element method was developed within the field of stress analysis and this reflected within the construction and nomenclature of the approach.

The finite volume method is based on forming a discretization from an integral form

of the model equations, and entails subdividing the domain in a number of finite volumes. Within each volume, the integral relationships are applied locally and so exact conservation withing each volume is achieved. The resulting expressions for the unknowns often appear similar to finite difference approximations and depending on the particular method chosen may be considered as a special case of either the finite difference or finite element techniques. With the emphasis of most fluid modeling problems being based on conservation principles, the finite volume methods has become more popular approach for general fluid flow problems

Setting up a numerical scheme therefore involves:

1. Selection of a discretization method for the equations in the model. This implies the selection between finite difference, finite volume, spectral or finite volume methods as well as selection of the order of accuracy of the spatial and eventually the time discretization.

2. Analysis of the selected numerical algorithm. This step concerns the analysis of the qualities of the scheme in terms of stability and convergence properties as well as the investigation of generated errors.

3. Selection of a resolution method for the system of ordinary/partial differential equations in time, for the algebraic system of equations and for the iterative treatment of eventual non-linearities.

We first take a look at numerical schemes that we have used in this thesis with respect

to how they are generally applied and some properties that make their applications wide in the area considered. Then the preceding sections give a general look at solving linear and non-linear algebraic systems of equations that come up with regards to finite difference equations.

3.1.1 Efficiency of a Numerical Scheme

There are four general ways to determine how well a particular numerical technique performs in generating results to a problem being modeled. These are accuracy, consistency, stability and convergence. The following are summaries of these characteristics.

Accuracy

This is the measure of how well discrete solutions represent the exact solution of the problem. We use the *local / truncation errors*; this measures how well the difference equations match the differential equations. We also use *global error* which reflects the overall error in the solution; possible only with the existence of an exact solution. An expression for the truncation error can be obtained by substituting the known exact solution of the problem into the discretization, leaving a remainder which is then a measure of the error.

Consistency

Consistency is related to adjusting grid resolution and its effect on the results. Mathematically, a method is said to be consistent if the truncation error decreases as the step

size is reduced which is the case when $q, p \geq 0$ This is equivalent to saying that as $\Delta t, \Delta x$ tends to zero, the discretized equations should tend towards the differential equations. It is necessary that a scheme be consistent for its practical use.

Stability

A numerical scheme is said to be stable if all of the errors such as round off errors due to finite arithmetic of the computer that exists within the solution are bounded. An unstable method results in a solution that tend towards infinity.Most methods have restrictions placed on the nature of their stability for example is the common use of the ratio of Δx to Δt plus a factor.

Convergence

Simply stated, convergence of a method refers to the ability of the method to approach the exact solutions as the grid spacing is reduced to zero. This is coupled with the global error.

Another very important criterion which must be satisfied in order to produce a valid solution is the issue of the particular problem being *well posed*. A problem is considered well posed if the following conditions are well met:

1. An existence of a solution
2. Uniqueness of the solution
3. A linear dependence of the solution on the data

The last condition can be translated to mean that the solution should not be sensitive to small changes in the initial / boundary data of the problem. If a problem is not well posed, then a valid numerical solution cannot be generated and any numerical treatment will either fail or produce poor results. Application of inappropriate boundary conditions is a way of producing an *ill-posed* problem.

3.1.2 Explicit and Implicit Formulations

A major division in numerical methods is considering whether a particular method is *explicit* or *implicit*.

If the solution is to be advanced to time level $n + 1$, the spatial derivatives may be approximated either in terms of the known values at time level n or the unknown quantities at time level $n + 1$.

An explicit method is generated from an approximation for the spatial derivatives using time level n. Put in a more mathematical way, for time dependent numerical formulations, the matrix of the unknown variables at the new time is a diagonal whiles the right hand side of the system is being dependent only on the flow variables in the previous times. This leads therefore to a trivial matrix inversion and hence to a solution with minimal number of arithmetic operations for each time step.

An implicit method on the other hand results from using the time level $n+1$ as approximations for the spatial derivatives. For time dependent formulations, this is a situation where the matrix to be inverted is not diagonal since more than one set of the variables

are unknown at the same time level.

Explicit methods are generally simpler in terms of the resulting algebraic equations as compared to implicit methods that require matrix inversions which turn out to be computationally costly. The advantage of implicit schemes lies in their independence of the times steps since most explicit methods turn out to be conditionally stable.

The next section is on finite difference schemes and their applications.

3.2 Finite Difference Schemes

The first application of this class of numerical methods is attributed to Leonard Euler (1707 - 1783) in 1768. This was the first technique to be developed for approximating ordinary differential equations from which theories regarding their properties and alternate applications in other subjects have been generated. This section gives a summary of finite difference methods.

The basis for finite difference methods is the expansion of Taylor Series and substitution of truncated expressions into the differntial equati. This can be applied to any structured mesh configuration.

Consider a function $u(x)$, the derivative at point x is simply defined by

$$u_x = \frac{du}{dx} = \lim_{x \to 0} = \frac{u(x + \Delta x) - u(x)}{\Delta x} \tag{3.1}$$

The removal of the limit in the above equation results in a finite difference, which explains the name given to it. When Δx is small this formula can be used as an approximation

for the derivative of u at x.

Then the numerical solution u_i can be thought of as point values where $u_i = u(i\Delta x)$. With reference to the notation discussed the approximate first derivative of u with respect to x can be written alternatively as:

1. Forward difference

$$(u_x)_i = \frac{u_{i+1} - u_i}{\Delta x} + O(\Delta x)$$

2. Backward difference

$$(u_x)_i = \frac{u_i - u_{i-1}}{\Delta x} + O(\Delta x)$$

3. Central difference

$$(u_x)_i = \frac{u_{i+1} - u_{i-1}}{2\Delta x} + O((\Delta x)^2)$$

These can all be used to approximate the first derivative of u with respect to x. In the area of truncation errors, the forward and backward differences are both first order approximations whereas the central difference is second order, as can be shown by Taylor series analysis. These formulae depends on the problem being modeled. In the case of PDEs for example which we will be taking particular look at, most schemes are based upon straight forward, backward and central difference formula.

The examples considered above therefore constitute the fundamental concepts that hold finite difference methods in place. The complexity that unfolds in this branch of computation is solely based on how these equations are proved. Considering u now as a function of two variables, i.e. $u(x,t)$, then the following are derivatives taken with respect to the independent variables and the associated errors attached to the derivatives. Considering

$u(x_i, t_j)$ and the fact that a value of $u(x,t)$ at a grid point (x_i, t_j) can be denoted by $u_i^j = u(x_i, t_j)$, we can write

1. Forward difference for u_x:
$$u_x(x_i, t_j) = \frac{u_{i+1}^j - u_i^j}{\Delta x} + O(\Delta x)$$

2. Backward difference for u_x:
$$u_x(x_i, t_j) = \frac{u_i^j - u_{i-1}^j}{\Delta x} + O(\Delta x)$$

3. Centered difference for u_x
$$u_x(x_i, t_j) = \frac{u_{i+1}^j - u_{i-1}^j}{2\Delta x} + O((\Delta x)^2)$$

4. Centered difference for u_{xx}
$$u_{xx}(x_i, t_j) = \frac{u_{i-1}^j - 2u_i^j + u_{i+1}^j}{(\Delta x)^2} + O((\Delta x)^2)$$

5. Forward difference for u_t:
$$u_t(x_i, t_j) = \frac{u_i^{j+1} - u_i^j}{\Delta t} + O(\Delta t)$$

6. Centered difference for u_t:
$$u_t(x_i, t_j) = \frac{u_i^{j+1} - u_i^{j-1}}{2\Delta t} + O((\Delta t)^2)$$

7. Centered difference for u_{tt}:
$$u_{tt}(x_i, t_j) = \frac{u_i^{j-1} - 2u_i^j + u_i^{j-1}}{(\Delta t)^2} + O((\Delta t)^2)$$

These formulae are most useful for solving PDEs. The notation used to represent the derivatives is known as the compact subscript-superscript and order of magnitude notation.

3.2.1 Application of Finite Difference Schemes to PDEs

Finite difference schemes are used to develop efficients methods for approximating solutions to partial differential equations. Suppose that a partial differential equation (PDE) is expressed symbolically as $L[u] = S$, holds on some region Ω of the $x - t$ plane. Let us cover with a finite difference grid $(x_i, t_j) = (i\Delta x, j\Delta t)$. The figure below is an illustration of the procedure. If all the derivatives in the PDE are replaced by difference quotients, the results is a *finite difference equation*(FDE). This is known as the method of *discretization* or *differencing* the continuous PDE problem to obtain a discrete FDE problem. Differencing therefore entails using difference quotients to approximate derivatives in the manner discussed.

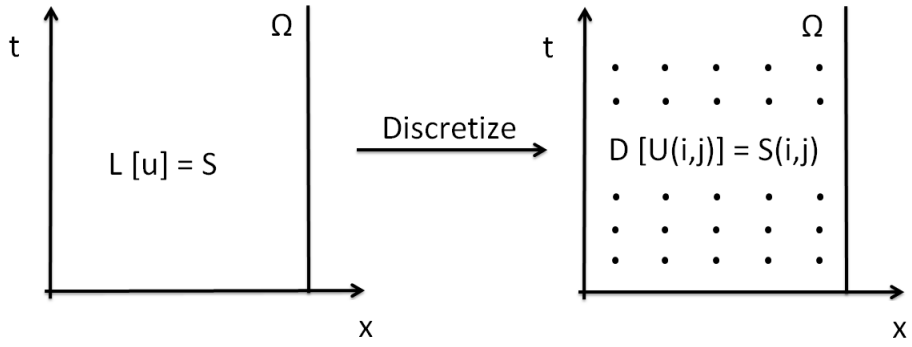

Figure 3.1: Conversion of a differential equation to a difference equation

The solution of the FDE U_i^j approximates $u_i^j = u(x_i, t_j)$, the solution of the PDE at the grid points. If the discretization is to provide a useful approximation, the solution of the PDE should nearly satisfy the FDE when the grid spacings Δx and Δt are taken sufficiently small. The conditions for efficiency of a numerical scheme should apply here.

3.3 Numerical Scheme for the Mathematical Models

This thesis takes into consideration the Preissmann scheme which is an implicit finite difference scheme. The researcher uses this weighted scheme to solve all the models discussed in this thesis.

3.3.1 Preissmann Scheme

The Preissmann scheme is the most widely applied implicit finite difference scheme because of its simple structure with both flow and geometrical variable in each grid point. This implies a simple treatment of boundary conditions and a simple incorporation of structure and bifurcation points. Also it has the advantages that steep wave fronts may be properly simulated by varying the weighting coefficient, α.

The scheme was first proposed by Alexander Preissmann in 1961 when he was a hydraulic engineer. It has been used since then for hydraulic modeling in various distinctions with the hydraulic setting. [Preissmann and Cunge 1961; Ligget and Cunge, 1965, Cunge, Holly and Versey, 1980]. Also known as the the box scheme, the reasons for it's widespread use are as follows:

- it works on non-staggered grid, which allows us to calculate both unknowns in the same nodes. This is important in natural rivers.
- it relates the variables coming from neighboring nodes only, what allows us using variable space interval Δx without affecting the accuracy of approximation.

- it ensures approximation of 1st order of accuracy and for particular case of 2nd order.
- it gives exact solution of the linear wave equations for properly chosen values of Δx and Δt, making possible the comparison of exact and numerical solutions.
- it is implicit and absolutely stable so it does not require limiting of the value of time step, whereas the imposed boundary conditions are introduced readily.

The four-point implicit Preissmann finite difference scheme uses a forward difference and weighted parameter, α as shown below:

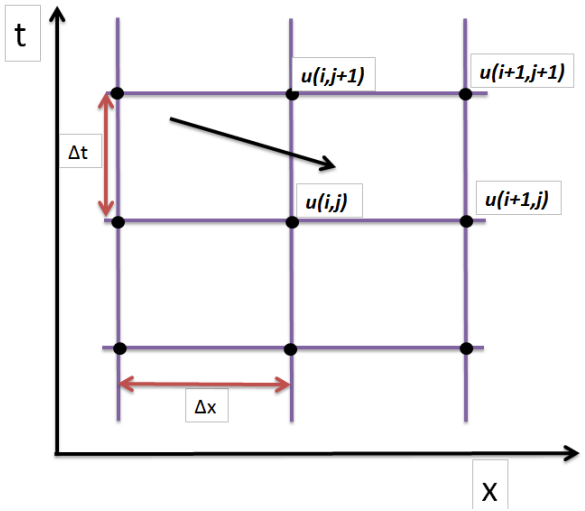

Figure 3.2: Computational stencil for the Preissmann scheme

A point u_p is therefore approximated as

$$u_p = \frac{1}{2}\left(\alpha u_i^{k+1} + (1-\alpha)u_i^k\right) + \frac{1}{2}\left(\alpha u_{i+1}^{k+1} + (1-\alpha)u_{i+1}^k\right)$$

with k, i begin the time and spatial indices respectively. The weighted parameter α lies

between 0 and 1. Derivatives are approximated as follows:

$$\begin{aligned}\frac{\partial u}{\partial t} &= \frac{\left(u_{i+1}^{k+1}+u_i^{k+1}\right)-\left(u_{i+1}^{k}+u_i^{k}\right)}{2\Delta t}\\ \frac{\partial u}{\partial x} &= \alpha\frac{\left(u_{i+1}^{k+1}-u_i^{k+1}\right)}{\Delta x}+(1-\alpha)\frac{\left(u_{i+1}^{k}-u_i^{k}\right)}{\Delta x}\end{aligned}$$

This scheme is second order if $\alpha = 0.5$, and first oder accurate otherwise. Linear stability analysis shows that the centered scheme is unconditionally stable for $\alpha \geq 0$. This feature makes it very interesting for practical applications, since contrarily to the case of explicit scheme, it is not subject to the Courant-Friedrichs-Levy stability condition that constraints the time to small values.

The Preissmann for these likely reasons has become the standard method for one-dimensional numerical modeling in the field of hydraulic engineering. A stability analysis including convective and friction terms has shown another condition is necessary however for the stability of the Preissmann scheme in addition to the conditions already discussed. The Vedernikov number γ, must be smaller than 1 where γ is defined by

$$\gamma = \frac{a}{b}\frac{A}{R}\frac{dR}{dA}F_0$$

where a is the exponent of the hydraulic radius and b the exponent of the velocity in the evaluation of the friction slope, A is the cross-sectional area of flow, R is the hydraulic radius and F_0 is the Froude number.

The Preissmann scheme is the discretization method used in the Institute for Software Integrated Systems (ISIS) package for the unsteady solver simulation which solves Saint Venant based equations for free surface flows(open channels)

3.4 Solution to Systems of Algebraic Equations

One of the very basic problems that occur in numerical analysis of partial differential equation with finite difference especially is the solution of linear systems of algebraic equations. Most times, nonlinear systems of partial differential equations are converted using existing methods of solution to linear systems of equations before they are solved. There exists two main branches of solution with regards to the subject of linear systems: i.e. *direct* methods and *iterative* methods. The sections that follow highlight general solution to system of equations and also discusses how to handle non-linear systems of equations by conversion to linear systems.

3.4.1 Linear Systems of Equations

Consider a system of n linear equations with n unknowns for which in matrix form we can write as

$$\mathbf{AX} = \mathbf{B} \tag{3.2}$$

where

$$\mathbf{A} = \begin{pmatrix} a_{11} & a_{12} & \cdots & a_{1n} \\ a_{21} & a_{22} & \cdots & a_{2n} \\ \vdots & \vdots & \ddots & \vdots \\ a_{n1} & a_{n2} & \cdots & a_{nn} \end{pmatrix} \quad \mathbf{X} = \begin{pmatrix} x_1 \\ x_2 \\ \vdots \\ x_n \end{pmatrix} \quad \mathbf{B} = \begin{pmatrix} b_1 \\ b_2 \\ \vdots \\ b_n \end{pmatrix}$$

where $\mathbf{A} = (a_{ij})$ $(i, j = 1, 2, \ldots, n)$ is a real square matrix of system coefficients,

$\mathbf{X} = (x_i)$ $(i = 1, 2, \ldots, n)$ is a column vector of unknowns and $\mathbf{B} = (b_i)$ $(i = 1, 2, \ldots, n)$ is a column vector of constants.

It is assumed that the matrix **A** is nonsingular so that the system (3.2) has a solution. The matrix **A** mostly occurs in practice as **diagonal matrices**, **lower triangular matrices**, **upper triangular matrices**,**sparse matrices**, **banded matrix** or in some cases **symmetric matrices**.

For the cases listed, advantage can be taken of the special structure of the matrix to generate solution algorithm much more efficient. The choice of either a whether to use a direct method or iterative method directly depends on these factors. The nature and size of the matrix are factors that influence the choice of methods of solution. Also important is the kind of solutions that these methods bring on board. Direct methods are capable of providing exact solutions after executing a finite number of mathematical operations (on condition that round off errors do not occur). Iterative methods on the other hand make use of an initial guess of the solution and provide a series of better approximations for the solution. In the process of doing this, if the series of solution that the iterative method present converges, i.e. if it tends to a limit, then the limit is referred to as the solution of the considered system.

3.4.2 Solution to Nonlinear System of Equations

For systems that are non-linear, there are a number of techniques available for the solution of the unknown vector. The methods of solution for non-linear systems are all iterative.

Consider a system of algebraic equations

$$\mathbf{AX} = \mathbf{B} \tag{3.3}$$

If in modeling a problem, this results in the coefficients matrix being functions of the unknowns i.e. $a_{ij} = a_{ij}(x_1, x_2, \ldots, x_n)$ or/and $b_i = b_i(x_1, x_2, \ldots, x_n)$, the system (3.3) is referred to as a *nonlinear* system. This is the occurrence as we will see when the Saint Venant equations are discretized using the four point Preissmann scheme. The nonlinear system of equation is usually represented by

$$\mathbf{F}(\mathbf{X}) = 0 \tag{3.4}$$

where

$$\begin{aligned} \mathbf{F}(\mathbf{X}) &= \mathbf{AX} - \mathbf{B} \\ \mathbf{X} &= (x_1, x_2, x_3, \ldots, x_n)^T \\ \mathbf{F} &= (f_1(x), f_2(x), f_3(x), \ldots, f_n(x))^T \end{aligned}$$

The following is a brief note on the Newton Method which is a standard method of solution for nonlinear systems.

Newton Method

Assume that the approximate solution of the nonlinear system is known. Then we can write

$$\mathbf{X} = \mathbf{X}^{(k)} + \Delta\mathbf{X}^{(k)} \tag{3.5}$$

where

$$\begin{aligned} \mathbf{X} &= \text{exact solution of the nonlinear of the system} \\ \mathbf{X}^{(k)} &= \text{solution approximation } \ i \ \text{ iteration } \ k \\ \Delta\mathbf{X}^{(k)} &= \text{vector of differences between the exact and estimate} \\ k &= \text{index of iteration} \end{aligned}$$

Assume that the functions being components of the system are *continuous* and differentiable with regards to $\mathbf{X}$. Using the fact the $\mathbf{F}(\mathbf{X}) = 0$ and using Taylor series expansion around $\mathbf{X}^{(k)}$, we obtain

$$\mathbf{F}\left(\mathbf{X}^{(k)} + \Delta\mathbf{X}^{(k)}\right) \approx \mathbf{F}\left(\mathbf{X}^{(k)}\right) + \frac{\partial\mathbf{F}\left(\mathbf{X}^{(k)}\right)}{\partial\mathbf{X}}\Delta\mathbf{X}^{(k)} \approx 0 \tag{3.6}$$

with the correction vector expressed as

$$\Delta\mathbf{X}^{(k)} = \mathbf{X}^{(k+1)} - \mathbf{X}^{(k)} \tag{3.7}$$

Since $\mathbf{X}^{(k)}$ estimates the exact solution $\mathbf{X}$. It is therefore possible to write:

$$\frac{\partial\mathbf{F}\left(\mathbf{X}^{(k)}\right)}{\partial\mathbf{X}}\left(\mathbf{X}^{(k+1)} - \mathbf{X}^{(k)}\right) = -\mathbf{F}\left(\mathbf{X}^{(k)}\right) \tag{3.8}$$

where

$$\frac{\partial\mathbf{F}\left(\mathbf{X}^{(k)}\right)}{\partial\mathbf{X}} = \mathbf{J}^{(k)} = \begin{bmatrix} \frac{\partial f_1\left(x_1^{(k)}, x_2^{(k)}, \ldots, x_n^{(k)}\right)}{\partial x_1} & \cdots & \frac{\partial f_1\left(x_1^{(k)}, x_2^{(k)}, \ldots, x_n^{(k)}\right)}{\partial x_n} \\ \frac{\partial f_2\left(x_1^{(k)}, x_2^{(k)}, \ldots, x_n^{(k)}\right)}{\partial x_1} & \cdots & \frac{\partial f_2\left(x_1^{(k)}, x_2^{(k)}, \ldots, x_n^{(k)}\right)}{\partial x_n} \\ \vdots & \ddots & \vdots \\ \frac{\partial f_n\left(x_1^{(k)}, x_2^{(k)}, \ldots, x_n^{(k)}\right)}{\partial x_1} & \cdots & \frac{\partial f_n\left(x_1^{(k)}, x_2^{(k)}, \ldots, x_n^{(k)}\right)}{\partial x_n} \end{bmatrix} \tag{3.9}$$

(3.9) is the Jacobian of the nonlinear system (3.4). Then the vector form of the Newton Method is given as:

$$\mathbf{X}^{(k+1)} = \mathbf{X}^{(k)} - \left(\mathbf{J}^{(k)}\right)^{-1} \mathbf{F}\left(\mathbf{X}^{(k)}\right) \tag{3.10}$$

Because of the time and memory consuming nature of this structure () i.e. the building of the Jacobian matrix of dimension $n \times n$ in each iteration and the inversion of the matrix, it is rather preferable to use the system given below:

$$\mathbf{J}^{(k)} \Delta \mathbf{X}^{(k)} = -\mathbf{F}^{(k)} \tag{3.11}$$

This system (3.11) is a linear system that can be solved in terms of the correction vector $\Delta \mathbf{X}^{(k)}$. Afterwards the new estimate of $\mathbf{X}$ is calculated as

$$\mathbf{X}^{(k+1)} = \mathbf{X}^{(k)} + \Delta \mathbf{X}^{(k)} \tag{3.12}$$

When the matrix $\mathbf{J}$ happens to be banded, the approach is more efficient as discussed under systems of linear of equations. Note that once the Jacobian matrix is inverted, it looses its banded form and has all non-zero elements.

3.5 Numerical Solution of Models

This section presents the solution to the discussed routing models using the Priessmann Scheme also known as the Box Scheme. They include solutions for the Burgers' Equation model (BEM), Kinematic Wave Equation (KWM), The proposed third order approximate model and the normalized Saint Venant Equations.

3.5.1 Burgers' Equation Model

The Burgers' equation is given by

$$\frac{\partial h}{\partial t} + (\alpha + \beta h)\frac{\partial h}{\partial x} - c\frac{\partial^2 h}{\partial t^2} = 0 \tag{3.13}$$

Using the box scheme the derivatives are given as follows:

$$\begin{aligned}
\frac{\partial h}{\partial t} &= \frac{1}{2\Delta t}\left(h_{i+1}^{k+1} + h_{i-1}^{k+1}\right) - \frac{1}{2\Delta t}\left(h_{i+1}^{k} + h_{i-1}^{k}\right) \\
\frac{\partial h}{\partial x} &= \frac{\theta}{\Delta x}\left(h_{i+1}^{k+1} - h_{i}^{k+1}\right) + \frac{(1-\theta)}{\Delta x}\left(h_{i+1}^{k} - h_{i}^{k}\right) \\
\frac{\partial^2 h}{\partial x^2} &= (1-\theta)\frac{h_{i+1}^{k} - 2h_{i}^{k} + h_{i-1}^{k}}{\Delta x^2} + \theta\frac{h_{i+1}^{k} - 2h_{i}^{k} + h_{i-1}^{k}}{\Delta x^2}
\end{aligned}$$

Substituting the derivatives into the BEM, we get

$$\begin{aligned}
h_i^{k+1} - h_i^k + \alpha\frac{\Delta t}{2}\left[(1-\theta)\frac{\left(h_{i+1}^k - h_{i-1}^k\right)}{\Delta x} + \theta\frac{\left(h_{i+1}^{k+1} - h_{i-1}^{k+1}\right)}{\Delta x}\right] + \\
\beta\frac{\Delta t}{2}\left[h_{i+1}^k h_{i+1}^{k+1} - h_{i-1}^k h_{i-1}^{k+1}\right] - \\
\gamma\frac{\Delta t}{\Delta x^2}\left[(1-\theta)\left(h_{i+1}^k - 2h_i^k + h_{i-1}^k\right) + \theta\left(h_{i+1}^{k+1} - 2h_i^{k+1} + h_{i-1}^{k+1}\right)\right] &= 0
\end{aligned}$$

$$\text{let} \qquad s = \frac{\gamma\Delta t}{\Delta x^2}, \qquad r = \frac{\Delta t}{\Delta x}$$

$$\begin{aligned}
h_i^{k+1} + h_i^k + \frac{\alpha r}{2}(1-\theta)\left(h_{i+1}^k - h_{i-1}^k\right) + \frac{\alpha r}{2}\theta\left(h_{i+1}^{k+1} - h_{i-1}^{k+1}\right) \\
+\frac{\beta r}{2}\left(h_{i+1}^k h_{i+1}^{k+1} - h_{i-1}^k h_{i-1}^{k+1}\right) \\
-s(1-\theta)\left(h_{i+1}^k - 2h_i^k + h_{i-1}^k\right) - s\theta\left(h_{i+1}^{k+1} - 2h_i^{k+1} + h_{i-1}^{k+1}\right) &= 0
\end{aligned}$$

This can be simplified further as

$$\begin{aligned}
\left(a_4 + a_6 h_{i-1}^k + a_9\right)h_{i+1}^{k+1} + \left(1 + a_0\right)h_i^{k+1} + \left(a_3 + a_5 h_{i+1}^k + a_9\right)h_{i+1}^{k+1} \\
= -\left(a_2 + a_7\right)h_{i-1}^k - \left(a_8 - 1\right)h_i^k - \left(a_1 + a_7\right)h_{i+1}^k
\end{aligned}$$

where the introduced variables are defined by

$$a_1 = \alpha r(1-\theta)/2 \qquad a_3 = \alpha\theta/2 \qquad a_5 = \beta r/2 \qquad a_7 = -s(1-\theta) \qquad a_9 = -s\theta$$

$$a_2 = -\alpha r(1-\theta)/2 \qquad a_4 = -\alpha\theta/2 \qquad a_6 = -\beta r/2 \qquad a_8 = 2s(1-\theta) \qquad a_0 = 2s\theta$$

$$
\begin{aligned}
a_j^n &= \left(a_4 + a_6 h_{i-1}^k + a_9\right) \\
b_j^n &= (1 + a_0) \\
c_j^n &= \left(a_3 + a_5 h_{i+1}^k + a_9\right) \\
d_j^n &= -\left(a_2 + a_7\right) h_{i-1}^k - \left(a_8 - 1\right) h_i^k - \left(a_1 + a_7\right) h_{i+1}^k
\end{aligned}
$$

then the result is a triangular system of equations as follows

$$
a_j^n h_{j-1}^{n+1} + b_j^n h_j^{n+1} + c_j^n h_{j+1}^{n+1} = d_j^n \tag{3.14}
$$

illustrated in matrix form as

$$
\begin{pmatrix}
\bullet & \bullet & & \\
\bullet & \bullet & \bullet & \\
 & \bullet & \bullet & \bullet \\
 & & \bullet & \bullet
\end{pmatrix}
\begin{pmatrix}
h_2^2 \\ h_3^2 \\ h_4^2 \\ h_5^1
\end{pmatrix}
=
\begin{pmatrix}
d_2^1 - a_2^1 h_1^2 \\ \bullet \\ \bullet \\ d_5^1 - c_5^1 h_6^2
\end{pmatrix} \tag{3.15}
$$

We solve this system using appropriate methods of solving systems of algebraic equations. The procedure is then repeated for calculations of h at $n = 2, 3, \ldots, 5$

3.5.2 The Proposed Equation

The third order equation equation model is given by

$$
\frac{\partial h}{\partial t} + (\alpha + \beta h)\frac{\partial h}{\partial x} - c\frac{\partial^2 h}{\partial t^2} + d\frac{\partial^3 h}{\partial t^3} = 0 \tag{3.16}
$$

Using the box scheme the derivatives are given as follows:

$$
\begin{aligned}
\frac{\partial h}{\partial t} &= \frac{1}{2\Delta t}\left(h_{i+1}^{k+1} + h_{i-1}^{k+1}\right) - \frac{1}{2\Delta t}\left(h_{i+1}^k + h_{i-1}^k\right) \\
\frac{\partial h}{\partial x} &= \frac{\theta}{\Delta x}\left(h_{i+1}^{k+1} - h_i^{k+1}\right) + \frac{(1-\theta)}{\Delta x}\left(h_{i+1}^k - h_i^k\right) \\
\frac{\partial^2 h}{\partial x^2} &= (1-\theta)\frac{h_{i+1}^k - 2h_i^k + h_{i-1}^k}{\Delta x^2} + \theta\frac{h_{i+1}^{k+1} - 2h_i^{k+1} + h_{i-1}^{k+1}}{\Delta x^2} \\
\frac{\partial^3 h}{\partial t^3} &= (1-\theta)\frac{h_{i+2}^k - 2h_{i+1}^k + 2h_{i-1}^k - h_{i-2}^k}{2\Delta x^3} + \theta\frac{h_{i+2}^{k+1} - 2h_{i+1}^{k+1} + 2h_{i-1}^{k+1} - h_{i-2}^{k+1}}{2\Delta x^3}
\end{aligned}
$$

Substituting the derivatives into the proposed third order equation model, we get

$$\begin{aligned} h_i^{k+1} - h_i^k + \alpha\frac{\Delta t}{2}\left[(1-\theta)\frac{\left(h_{i+1}^k - h_{i-1}^k\right)}{\Delta x} + \theta\frac{\left(h_{i+1}^{k+1} - h_{i-1}^{k+1}\right)}{\Delta x}\right] + \\ \beta\frac{\Delta t}{2}\left[h_{i+1}^k h_{i+1}^{k+1} - h_{i-1}^k h_{i-1}^{k+1}\right] - \\ \gamma\frac{\Delta t}{\Delta x^2}\left[(1-\theta)\left(h_{i+1}^k - 2h_i^k + h_{i-1}^k\right) + \theta\left(h_{i+1}^{k+1} - 2h_i^{k+1} + h_{i-1}^{k+1}\right)\right] \\ +\frac{d\Delta t}{3\Delta x^3}\left[(1-\theta)\frac{h_{i+2}^k - 2h_{i+1}^k + 2h_{i-1}^k - h_{i-2}^k}{2\Delta x^3} + \theta\frac{h_{i+2}^{k+1} - 2h_{i+1}^{k+1} + 2h_{i-1}^{k+1} - h_{i-2}^{k+1}}{2\Delta x^3}\right] &= 0 \end{aligned}$$

$$\text{let} \qquad s = \frac{\gamma\Delta t}{\Delta x^2}, \qquad r = \frac{\Delta t}{\Delta x} \qquad p = \frac{d\Delta t}{2\Delta x^3}$$

$$\begin{aligned} h_i^{k+1} + h_i^k + \frac{\alpha r}{2}(1-\theta)\left(h_{i+1}^k - h_{i-1}^k\right) + \frac{\alpha r}{2}\theta\left(h_{i+1}^{k+1} - h_{i-1}^{k+1}\right) \\ +\frac{\beta r}{2}\left(h_{i+1}^k h_{i+1}^{k+1} - h_{i-1}^k h_{i-1}^{k+1}\right) \\ -s(1-\theta)\left(h_{i+1}^k - 2h_i^k + h_{i-1}^k\right) - s\theta\left(h_{i+1}^{k+1} - 2h_i^{k+1} + h_{i-1}^{k+1}\right) \\ +p\left[\theta(h_{i+2}^{k+1} - h_{i+1}^{k+1} + 2h_{i-1}^{k+1} - h_{i-2}^{k+1}) + (1-\theta)(h_{i+2}^k - h_{i+1}^k + 2h_{i-1}^k - h_{i-2}^k)\right] &= 0 \end{aligned}$$

This can be simplified further as

$$\begin{aligned} b_4 h_{i-2}^{k+1} + \left(b_3 + a_9 + a_4 + a_6 h_{i-1}^k\right) h_{i+1}^{k+1} + \left(1 + a_0\right) h_i^{k+1} + \left(b_2 + a_3 + a_9 + a_5 h_{i+1}^k\right) h_{i+1}^{k+1} + b_1 h_{i+2}^{k+1} \\ = -b_8 h_{i-2}^k - \left(b_7 + a_2 + a_7\right) h_{i-1}^k - \left(a_8 - 1\right) h_i^k - \left(b_6 + a_1 + a_7\right) h_{i+1}^k - b_5 h_{i+2}^k \end{aligned}$$

where the introduced variables are defined by

$a_1 = \alpha r(1-\theta)/2$	$a_3 = \alpha\theta/2$	$a_5 = \beta r/2$	$a_7 = -s(1-\theta)$	$a_9 = -s\theta$
$a_2 = -\alpha r(1-\theta)/2$	$a_4 = -\alpha\theta/2$	$a_6 = -\beta r/2$	$a_8 = 2s(1-\theta)$	$a_0 = 2s\theta$
$b_1 = p\theta$	$b_2 = -2p\theta$	$b_3 = 2p\theta$	$b_4 = -p\theta$	
$b_5 p(1-theta)$	$b_6 = -2p(1-\theta)$	$b_7 = 2p(1-\theta)$	$b_8 = -p(1-\theta)$	

$$
\begin{aligned}
x_0^k &= b_4 & x_1^k &= \left(b_3 + a_4 + a_9 + a_6 h_{i-1}^k\right) \\
x_2^k &= (1 + a_0) & x_3^k &= \left(b_2 + a_3 + a_9 + a_5 h_{i+1}^k\right) \\
x_4^k &= b_1 & x_5^k &= -b_8 \\
x_6^k &= -(b_7 + a_7 + a_2) & x_7^k &= 1 - a_8 \\
x_8^k &= -(b_6 + a_7 + a_1) & x_9^k &= -b_5 \\
& & d_i^k &= x_5^k h_{i-2}^k + x_6^k h_{i-1}^k + x_7^k h_i^k + x_8^k h_{i+1}^k + x_9^k h_{i-2}^k
\end{aligned}
$$

then the implicit system can be written as

$$
x_0^n h_{i-2}^{k+1} + x_1^n h_{i-1}^{k+1} + x_2^n h_i^{k+1} + x_3^n h_{i+1}^{k+1} + x_4^n h_{i+2}^{k+1} = d_j^n \tag{3.17}
$$

Expressed in matrix form, a system of 8 unknowns will conform to

$$
\begin{pmatrix}
\bullet & \bullet & \bullet & & & & & \\
\bullet & \bullet & \bullet & \bullet & & & & \\
\bullet & \bullet & \bullet & \bullet & \bullet & & & \\
 & \bullet & \bullet & \bullet & \bullet & \bullet & & \\
 & & \bullet & \bullet & \bullet & \bullet & & \\
 & & & \bullet & \bullet & \bullet & & \\
 & & & & & & & \\
 & & & & & & &
\end{pmatrix}
\begin{pmatrix} h_3^2 \\ h_4^2 \\ h_5^1 \\ h_6^2 \\ h_7^2 \\ h_8^2 \end{pmatrix}
=
\begin{pmatrix} d_3^2 - x_0^1 h_1^2 - x_1^1 h_2^2 \\ d_4^2 - x_0^2 h_2^2 \\ \bullet \\ \bullet \\ d_7^2 - x_4^5 h_{10}^2 \\ d_8^2 - x_3^6 h_9^2 - x_4^6 h_{10}^2 \end{pmatrix} \tag{3.18}
$$

We solve this system using appropriate methods of solving systems of algebraic equations. The procedure is then repeated for calculations of h at $n = 2, 3, \ldots, 10$

3.5.3 Kinematic Wave Equation

Using the Preissmann implicit scheme, we approximate the derivatives and points as follows:

$$
\begin{aligned}
\frac{\partial h}{\partial t} &= \frac{1}{2\Delta t}\left(h_{i+1}^{k+1} + h_i^{k+1}\right) - \frac{1}{2\Delta t}\left(h_{i+1}^k + h_i^k\right) \\
\frac{\partial h}{\partial x} &= \frac{\alpha}{\Delta x}\left(h_{i+1}^{k+1} - h_i^{k+1}\right) + \frac{(1-\alpha)}{\Delta x}\left(h_{i+1}^k - h_i^k\right) \\
h_p &= \frac{\alpha}{2}\left(h_{i+1}^{k+1} + h_i^{k+1}\right) + \frac{(1-\alpha)}{2}\left(h_{i+1}^k + h_i^k\right)
\end{aligned}
$$

By substituting these derivatives into the the KWM we have

$$c_1 h_i^{k+1} + c_2 h_{i+1}^{k+1} + \left[a_3 h_{i+1}^{k+1} + a_4 h_i^{k+1} + a_5 h_{i+1}^{k} + a_6 h_i^{k}\right] b h_p + c_3 h_i^{k} + c_4 h_{i+1}^{k} = 0 \tag{3.19}$$

where

$$\begin{aligned} a_1 &= \Delta x \qquad a_3 = 2\alpha\Delta t \qquad a_5 = 2(1-\alpha)\Delta t \\ a_2 &= -\Delta x \qquad a_4 = -2\alpha\Delta t \qquad a_6 = -2(1-\alpha)\Delta t \end{aligned} \tag{3.20}$$

and

$$\begin{aligned} c_1 &= (a_1 + a a_4) \qquad c_3 = (a_2 + a a_6) \\ c_2 &= (a_1 + a a_3) \qquad c_4 = (a_2 + a a_5) \end{aligned} \tag{3.21}$$

This is a nonlinear system which can be solved using the Newton Method.

We therefore find the Jacobian matrix associated with a system of equations of for example $k = 1:6$. It is given by a lower triangular matrix

$$\mathbf{J} = \begin{pmatrix} J_{11} & & & & \\ J_{21} & J_{22} & & & \\ & J_{32} & J_{33} & & \\ & & J_{43} & J_{44} & \\ & & & J_{54} & J_{55} \end{pmatrix} \tag{3.22}$$

The unknown vector $\mathbf{X}$ which contains the unknown variables is solved in the system

$$\mathbf{J^k \Delta X} = -\mathbf{F^k} \tag{3.23}$$

where

$$\mathbf{X} = \begin{pmatrix} h_2^2 \\ h_3^2 \\ h_4^2 \\ h_5^2 \\ h_6^2 \end{pmatrix}; \qquad \mathbf{F} = \begin{pmatrix} F_1\left(h_2^2, h_3^2, h_4^2, h_5^2, h_6^2\right) \\ F_2\left(h_2^2, h_3^2, h_4^2, h_5^2, h_6^2\right) \\ F_3\left(h_2^2, h_3^2, h_4^2, h_5^2, h_6^2\right) \\ F_4\left(h_2^2, h_3^2, h_4^2, h_5^2, h_6^2\right) \\ F_5\left(h_2^2, h_3^2, h_4^2, h_5^2, h_6^2\right) \end{pmatrix} \tag{3.24}$$

3.5.4 Saint Venant Equations

The numerical solution of the Saint Venant Equations is discretized as follows: First the continuity equation is considered-

$$\frac{\partial h}{\partial t} + \frac{\partial (uh)}{\partial x} = 0 \tag{3.25}$$

Using the Preissmann scheme the partial derivative of a variable with respect to x and t are given as follows

$$\frac{\partial h}{\partial x} = \alpha \frac{\left(h_{i+1}^{k+1} - h_i^{k+1}\right)}{\Delta x} + (1-\alpha)\frac{\left(h_{i+1}^{k} - h_i^{k}\right)}{\Delta x} \tag{3.26}$$

$$\frac{\partial h}{\partial t} = \frac{1}{2}\frac{\left(h_{i}^{k+1} + h_{i+1}^{k+1}\right)}{\Delta t} - \frac{1}{2}\frac{\left(h_{i}^{k} + h_{i+1}^{k}\right)}{\Delta t} \tag{3.27}$$

Substituting these finite difference into the continuity equation and arranging coefficients of similiar terms we have

$$\begin{aligned} &\phi_{11}h_i^{k+1} + \phi_{12}u_i^{k+1} + \phi_{13}h_{i+1}^{k+1} + \phi_{14}u_{i+1}^{k+1} \\ &+\mu_{11}h_i^k + \mu_{12}u_i^k + \mu_{13}h_{i+1}^k + \mu_{14}u_{i+1}^k = 0 \end{aligned}$$

where the introduced constants in the problem are defined as follows :

$$\begin{aligned} a_1 &= \Delta x & a_3 &= 2\alpha\Delta t & a_5 &= 2(1-\alpha)\Delta t \\ a_2 &= -\Delta x & a_4 &= -2\alpha\Delta t & a_6 &= -2(1-\alpha)\Delta t \end{aligned} \tag{3.28}$$

and

$$\begin{aligned} \phi_{11} &= a_1 & \phi_{13} &= a_1 & \mu_{11} &= a_2 & \mu_{13} &= a_2 \\ \phi_{12} &= a_4 h_i^{k+1} & \phi_{14} &= a_3 h_{i+1}^{k+1} & \mu_{12} &= a_6 h_i^k & \mu_{14} &= a_5 h_{i+1}^k \end{aligned} \tag{3.29}$$

From the momentum equation, we have

$$\frac{\partial u}{\partial t} + u\frac{\partial u}{\partial x} + \frac{\partial h}{\partial x} + \frac{1}{F_0^2}\frac{u^2}{h^{2m}} - 1 = 0 \tag{3.30}$$

Taking the derivatives in the equation and using the Preissmann scheme to discretize them and then finally subsituting them into the momentum equation (3.30), we have

$$\begin{aligned} &\phi_{21}h_i^{k+1} + \phi_{22}u_i^{k+1} + \phi_{23}h_{i+1}^{k+1} + \phi_{24}u_{i+1}^{k+1} \\ &+\mu_{21}h_i^k + \mu_{22}u_i^k + \mu_{23}h_{i+1}^k + \mu_{24}u_{i+1}^k + f_i \quad = \quad 0 \end{aligned}$$

where the introduced constants are given by

$$\begin{array}{lll} \phi_{21} = a_4 h_p^{2m} & \phi_{22} = (a_1 + a_4 u_p)\, h_p^{2m} & \phi_{23} = a_3 h_p^{2m} \\ \phi_{24} = (a_1 + a_4 u_p)\, h_p^{2m} & \mu_{21} = a_6 h_p^{2m} & \mu_{22} = (a_2 + a_6 u_p)\, h_p^{2m} \\ \mu_{23} = a_5 h_p^{2m} & \mu_{24} = (a_2 + a_5 u_p)\, h_p^{2m} & a_7 = \frac{1}{F_0^2} 2\Delta t \Delta x \\ a_8 = -2\Delta t \Delta x & f_i = a_7 u_p^2 + a_8 h_p^{2m} & \end{array} \tag{3.31}$$

The general scheme therefore is to solve the system of equations below

$$\begin{aligned} \phi_{11}h_i^{k+1} + \phi_{12}u_i^{k+1} + \phi_{13}h_{i+1}^{k+1} + \phi_{14}u_{i+1}^{k+1} + \mu_{11}h_i^k + \mu_{12}u_i^k + \mu_{13}h_{i+1}^k + \mu_{14}u_{i+1}^k \quad &= \quad 0 \\ \phi_{21}h_i^{k+1} + \phi_{22}u_i^{k+1} + \phi_{23}h_{i+1}^{k+1} + \phi_{24}u_{i+1}^{k+1} + \mu_{21}h_i^k + \mu_{22}u_i^k + \mu_{23}h_{i+1}^k + \mu_{24}u_{i+1}^k \quad &= \quad -f_i \end{aligned}$$

In the system of equations, the nodal values of the water levels h_i^{k+1} and h_{i+1}^{k+1} as well as the flow velocities u_i^{k+1} and u_{i+1}^{k+1} are unknowns.

Given the way they appear, a pair of equations can be written for each space interval for $i = 2, 3, \ldots, m-1$ where m here is the number of nodes in the spatial computation. We then obtain a set of $2(m-1)$ algebraic equations with $2m$ unknowns representing the nodal values of the function h and u. Two boundary conditions allow us to complete the system of equations. for $i = 2$

$$\delta_0 h_2^{k+1} + (1-\delta_0)h_2^{k+1} = \delta_0 h_1(t_{n+1}) + (1-\delta_0)u_1(t_{n+1}) \tag{3.32}$$

for $i = m-1$

$$\delta_L h_{m-1}^{k+1} + (1-\delta_L)h_{m-1}^{k+1} = \delta_L h_m(t_{n+1}) + (1-\delta_L)u_m(t_{n+1}) \tag{3.33}$$

In the above equations δ_0 and δ_L are integer values that can take values of 0 or 1. The value of 1 designates the boundary condition imposed in the form of water stage (function $h_1(t)$ or $h_m(t)$) whereas the value of 0 corresponds to the flow velocity (function $u_1(t)$ or $u_m(t)$). In this research, we use the water stage condition

For example, given an equally spaced grid with 6 nodes, we start with the calculation of the time driven unknowns $h_i^{k+1}, u_i^{k+1}, h_{i+1}^{k+1}$ and u_{i+1}^{k+1} as follows:

for $k = 1$, for $j = 2$

$$\begin{aligned}
\phi_{11}h_2^2 + \phi_{12}u_2^2 + \phi_{13}h_3^2 + \phi_{14}u_3^2 + \mu_{11}h_2^1 + \mu_{12}u_2^1 + \mu_{13}h_3^1 + \mu_{14}u_3^1 &= 0 \\
\phi_{21}h_2^2 + \phi_{22}u_2^2 + \phi_{23}h_3^2 + \phi_{24}u_3^2 + \mu_{21}h_2^1 + \mu_{22}u_2^1 + \mu_{23}h_3^1 + \mu_{24}u_3^1 &= -f
\end{aligned}$$

for $j = 3$

$$\begin{aligned}
\phi_{11}h_3^2 + \phi_{12}u_3^2 + \phi_{13}h_4^2 + \phi_{14}u_4^2 + \mu_{11}h_3^1 + \mu_{12}u_3^1 + \mu_{13}h_4^1 + \mu_{14}u_4^1 &= 0 \\
\phi_{21}h_3^2 + \phi_{22}u_3^2 + \phi_{23}h_4^2 + \phi_{24}u_4^4 + \mu_{21}h_3^1 + \mu_{22}u_3^1 + \mu_{23}h_4^1 + \mu_{24}u_4^4 &= -f
\end{aligned}$$

for $j = 4$

$$\begin{aligned}
\phi_{11}h_4^2 + \phi_{12}u_4^2 + \phi_{13}h_5^2 + \phi_{14}u_5^2 + \mu_{11}h_4^1 + \mu_{12}u_4^1 + \mu_{13}h_5^1 + \mu_{14}u_5^1 &= 0 \\
\phi_{21}h_4^2 + \phi_{22}u_4^2 + \phi_{23}h_5^2 + \phi_{24}u_5^2 + \mu_{21}h_4^1 + \mu_{22}u_4^1 + \mu_{23}h_5^1 + \mu_{24}u_5^1 &= -f
\end{aligned}$$

There are a total of 6 equations with 8 unknowns i.e. $h_2^2, u_2^2, h_3^2, u_3^2, h_4^2, u_4^2, h_5^2$ and u_5^2. In order to resolve this we expand the equation at the boundary conditions using the water stage conditions i.e. $\delta_0 = 1$ and $\delta_L = 0$. This gives us the two additional equations to complete the solution. The additional equations are given by

$$\begin{aligned}
\text{for } j = 2; h_2^2 &= h_1^2 \\
\text{for } j = 5; h_5^2 &= h_6^2
\end{aligned}$$

Adding the two boundary conditions, we have the system of equations in the form:

$$
\begin{aligned}
h_2^2 - h_1^2 &= 0 \\
\phi_{11}h_2^2 + \phi_{12}u_2^2 + \phi_{13}h_3^2 + \phi_{14}u_3^2 + \mu_{11}h_2^1 + \mu_{12}u_2^1 + \mu_{13}h_3^1 + \mu_{14}u_3^1 &= 0 \\
\phi_{21}h_2^2 + \phi_{22}u_2^2 + \phi_{23}h_3^2 + \phi_{24}u_3^2 + \mu_{21}h_2^1 + \mu_{22}u_2^1 + \mu_{23}h_3^1 + \mu_{24}u_3^1 &= -f \\
\phi_{11}h_3^2 + \phi_{12}u_3^2 + \phi_{13}h_4^2 + \phi_{14}u_4^2 + \mu_{11}h_3^1 + \mu_{12}u_3^1 + \mu_{13}h_4^1 + \mu_{14}u_4^1 &= 0 \\
\phi_{21}h_3^2 + \phi_{22}u_3^2 + \phi_{23}h_4^2 + \phi_{24}u_4^2 + \mu_{21}h_3^1 + \mu_{22}u_3^1 + \mu_{23}h_4^1 + \mu_{24}u_4^1 &= -f \\
\phi_{11}h_4^2 + \phi_{12}u_4^2 + \phi_{13}h_5^2 + \phi_{14}u_5^2 + \mu_{11}h_4^1 + \mu_{12}u_4^1 + \mu_{13}h_5^1 + \mu_{14}u_5^1 &= 0 \\
\phi_{21}h_4^2 + \phi_{22}u_4^2 + \phi_{23}h_5^2 + \phi_{24}u_5^2 + \mu_{21}h_4^1 + \mu_{22}u_4^1 + \mu_{23}h_5^1 + \mu_{24}u_5^1 &= -f \\
h_5^2 - h_6^2 &= 0
\end{aligned}
$$

In matrix form, we can write the system of equations above as

$$
\begin{pmatrix}
1 & 0 & 0 & 0 & 0 & 0 & 0 & 0 \\
\phi_{11} & \phi_{12} & \phi_{13} & \phi_{14} & 0 & 0 & 0 & 0 \\
\phi_{21} & \phi_{22} & \phi_{23} & \phi_{24} & 0 & 0 & 0 & 0 \\
0 & 0 & \phi_{11} & \phi_{12} & \phi_{13} & \phi_{14} & 0 & 0 \\
0 & 0 & \phi_{21} & \phi_{22} & \phi_{23} & \phi_{24} & 0 & 0 \\
0 & 0 & 0 & 0 & \phi_{11} & \phi_{12} & \phi_{13} & \phi_{14} \\
0 & 0 & 0 & 0 & \phi_{21} & \phi_{22} & \phi_{23} & \phi_{24} \\
0 & 0 & 0 & 0 & 0 & 0 & 1 & 0
\end{pmatrix}
\begin{pmatrix}
h_2^2 \\ u_2^2 \\ h_3^2 \\ u_3^2 \\ h_4^2 \\ u_4^2 \\ h_5^2 \\ u_5^2
\end{pmatrix} +
$$

$$\begin{pmatrix} 0 & 0 & 0 & 0 & 0 & 0 & 0 & 0 \\ \mu_{11} & \mu_{12} & \mu_{13} & \mu_{14} & 0 & 0 & 0 & 0 \\ \mu_{21} & \mu_{22} & \mu_{23} & \mu_{24} & 0 & 0 & 0 & 0 \\ 0 & 0 & \mu_{11} & \mu_{12} & \mu_{13} & \mu_{14} & 0 & 0 \\ 0 & 0 & \mu_{21} & \mu_{22} & \mu_{23} & \mu_{24} & 0 & 0 \\ 0 & 0 & 0 & 0 & \mu_{11} & \mu_{12} & \mu_{13} & \mu_{14} \\ 0 & 0 & 0 & 0 & \mu_{21} & \mu_{22} & \mu_{23} & \mu_{24} \\ 0 & 0 & 0 & 0 & 0 & 0 & 0 & 0 \end{pmatrix} \begin{pmatrix} h_2^1 \\ u_2^1 \\ h_3^1 \\ u_3^1 \\ h_4^1 \\ u_4^1 \\ h_5^1 \\ u_5^1 \end{pmatrix} = \begin{pmatrix} h_2^1 \\ 0 \\ -f \\ 0 \\ -f \\ 0 \\ -f \\ h_6^2 \end{pmatrix}$$

We can alternatively represent the system by

$$\mathbf{G}(\mathbf{X}) = \mathbf{A}\mathbf{X}^{(k+1)} + \mathbf{B}\mathbf{X}^{(k)} + \mathbf{F} = 0 \tag{3.34}$$

The system $\mathbf{G}(\mathbf{X})$ is nonlinear in terms of the unknown vector $\mathbf{X}^{k+1}$. Therefore we implement an iterative scheme. For this purpose we use the Newton method presented in earlier sections. The iteration process has the following form:

$$\mathbf{J}^{(k)}\Delta\mathbf{X}^{(k+1)} = -\mathbf{G}^{(k)} \tag{3.35}$$

where

$$\begin{aligned} \Delta\mathbf{X}^{(k+1)} = \mathbf{X}^{(k+1)} - \mathbf{X}^{(k)} \quad &- \quad \text{correction vector} \\ \mathbf{J}^{(k)} \quad &- \quad \text{Jacobian matrix} \\ k \quad &- \quad \text{index of iteration} \end{aligned}$$

The Newton method requires that the system of linear algebraic equations is solved in each iteration. To this purpose a modified Gauss elimination or **LU** decomposition algorithm should be used, which takes advantage of the banded matrix.

3.6 Efficiency Criteria

There are many efficiency criteria for measuring the margin of error between observed variables and predicted values by mathematical models. Whether the observed values are real catchment or are in themselves variables from existing models, established efficiency criteria can be used to compare the observed and predicted values.P. Krause and F. (2005)

Efficiency criteria are defined as mathematical measures of how well a model simulation fits available observations Beven (2001). In this thesis, the researcher makes use of the Coefficient of determination r^2, the Nash-Sutcliffe efficiency E, the index of agreement d, Nash-Sutcliffe efficiency with logarithmic value ln E, Modified forms of E and d and Relative efficiency criteria E_{rel} and d_{rel}. The Coefficient of determination r^2 is the squared of value of the coeffcient of correlation and ranges between which means no correlation and 1 where is a perfect correlation between observed and predicted values. The Nash-Sutcliffe, E measures performance for values between 1.0 (perfect fit) and $-\infty$ using 1 minus the sum of absolute squared difference between predicted and observed values. Both r^2 and E are insensitive to over- or underprediction. The efficiency criteria that overcomes the sensitivity to over-underprediction is the index of agreement, d. It has a range similar to r^2 with 0 (no correlation) and 1 (perfect fit). The formulae for the different efficiency criteria used in this research are defined mathematically in the below as: The following are formula for efficiency criteria used in this thesis. The symbols O and P used to calculate the different represnt the Observed values and Predicated values respectively.

3.6.0.1 Coefficient of Determination r^2

$$r^2 = \left(\frac{\sum_{i=1}^{n} \left(O_i - \bar{O}\right)\left(P_i - \bar{P}\right)}{\sqrt{\sum_{i=1}^{n} \left(O_i - \bar{O}\right)} \sqrt{\sum_{i=1}^{n} \left(P_i - \bar{P}\right)}} \right)^2 \tag{3.36}$$

3.6.0.2 Nash-Sutcliffe efficiency E

$$E = 1 - \frac{\sum_{i=1}^{n} \left(O_i - P_i\right)^2}{\sum_{i=1}^{n} \left(O_i - \bar{O}\right)^2} \tag{3.37}$$

3.6.0.3 Index of Agreement d

$$d = 1 - \frac{\sum_{i=1}^{n} \left(O_i - P_i\right)^2}{\sum_{i=1}^{n} \left(\left|P_i - \bar{O}\right| + \left|O_i - \bar{O}\right|\right)^2} \tag{3.38}$$

3.6.0.4 Modified forms of E and d

$$E_j = 1 - \frac{\sum_{i=1}^{n} \left|O_i - P_i\right|^j}{\sum_{i=1}^{n} \left|O_i - \bar{O}\right|^j} \quad \text{with } j \in \mathbf{N} \tag{3.39}$$

$$d_j = 1 - \frac{\sum_{i=1}^{n} \left|O_i - P_i\right|^j}{\sum_{i=1}^{n} \left(\left|P_i - \bar{O}\right| + \left|O_i - \bar{O}\right|\right)^j} \quad \text{with } j \in \mathbf{N} \tag{3.40}$$

3.6.0.5 Relative efficiency criteria E_{rel} and d_{rel}

$$E_{rel} = 1 - \frac{\sum_{i=1}^{n} \left(\frac{O_i - P_i}{O_i}\right)^2}{\sum_{i=1}^{n} \left(\frac{O_i - \bar{O}}{\bar{O}}\right)^2} \tag{3.41}$$

$$d_{rel} = 1 - \frac{\sum_{i=1}^{n} \left(\frac{O_i - P_i}{O_i}\right)^2}{\sum_{i=1}^{n} \left(\frac{\left|P_i - \bar{O}\right| + \left|O_i - \bar{O}\right|}{\bar{O}}\right)^2} \tag{3.42}$$

Chapter 4

Simulation Results and Discussion

4.1 Introduction

This chapter is a presentation of the simulation using the algorithms based on the implicit Preissmann scheme that has been used to solve the normalized Saint Venant Equations (SVE), the Burgers' Equation Model (BEM), the Kinematic Wave Equation (KWM) and the presented third order approximate model to the Saint Venant Equations. The algorithms have been programmed using MATrix LABoratory (MATLAB 7.8.0 (R2007a)) together with the formulas used for the efficiency criteria.

Using graphical techniques, the researcher visually examines the approximate models and the nature of solutions as compared to the SVE. The Graphical Technique provide a visual comparison of simulated and measured constituent data and first overview of model performance (ASCE, 1993)

Additionally, since the third order approximate model is an upgrade of the Burgers' Equation model, both models are compared graphically. The two approximate models (The BEM and the third order approximate model) are also evaluated using relative percentage deviations from the SVE. The researcher investigates the effect of the weighted parameter

that is found in the Preissmann scheme and its variational effect on the hydraulic models considered in this research. The limits of the flow depth difference (the difference between the initial and final flow depth) within which each of the models discussed in this thesis generate acceptable results are also investigated.

Finally, the researcher uses efficiency criteria to test the efficiency of the approximate models as compared to how well they mimic the parent model. The efficiency criteria are used to support the quantitative analysis.

4.1.1 Application

The hydraulic models presented in this research and the numerical algorithms provided in Section (3.5 - 3.7) have been applied to a series of hypothetical examples, simulating mainly the flow depth, h within considered distance and duration in a flow channel.

We consider the problem of a *Dam Break* and use the hydraulic models presented to simulate flow in this occurrence. A dam break refers to any problem where a barrier separating water at two different levels is suddenly removed. This can also be likened to the experiment of the sudden opening of a sluice or gate. The main objective in a dam break is to determine flow which results from a sudden destruction of the dam. The water is assumed to be at rest on both sides of the dam initially. At $t = 0$, the dam breaks and our problem is to determine the subsequent motion of the water for all x and t.

Fig. 4.1 and Fig4.2 are two situations that occur when water is staged at two different levels. Suppose that a rectangular canal having a horizontal bed with an initial depth,

$h_{initial}$ is contained by a lock or wall. If the lock gate or wall is suddenly removed, Fig. 1 displays the physical plane at time t for the propagation. The water level moves from the initial depth, $h_{initial}$ indicated in the diagram to a final depth, h_{final}.

If however, the gate or wall is removed relatively further and faster (instantaneously), the water level moves to the floor bed before it rises to the final depth, h_{final}. The description is captured in Fig 4.2 on page 54.

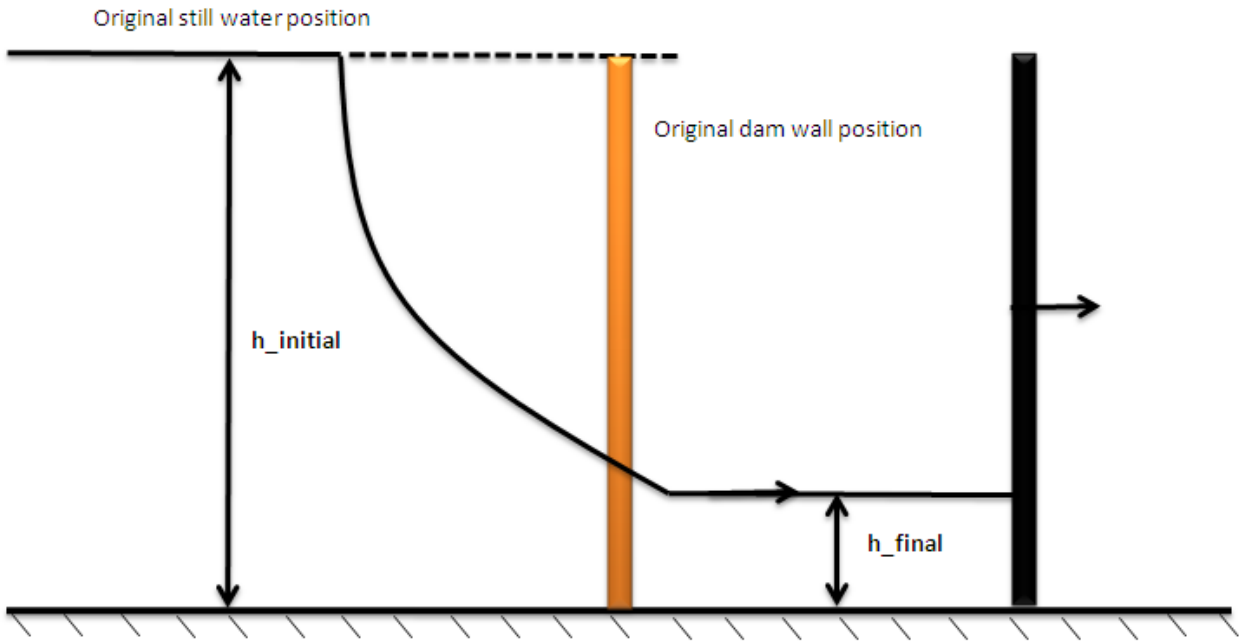

Figure 4.1: physical plane at time t

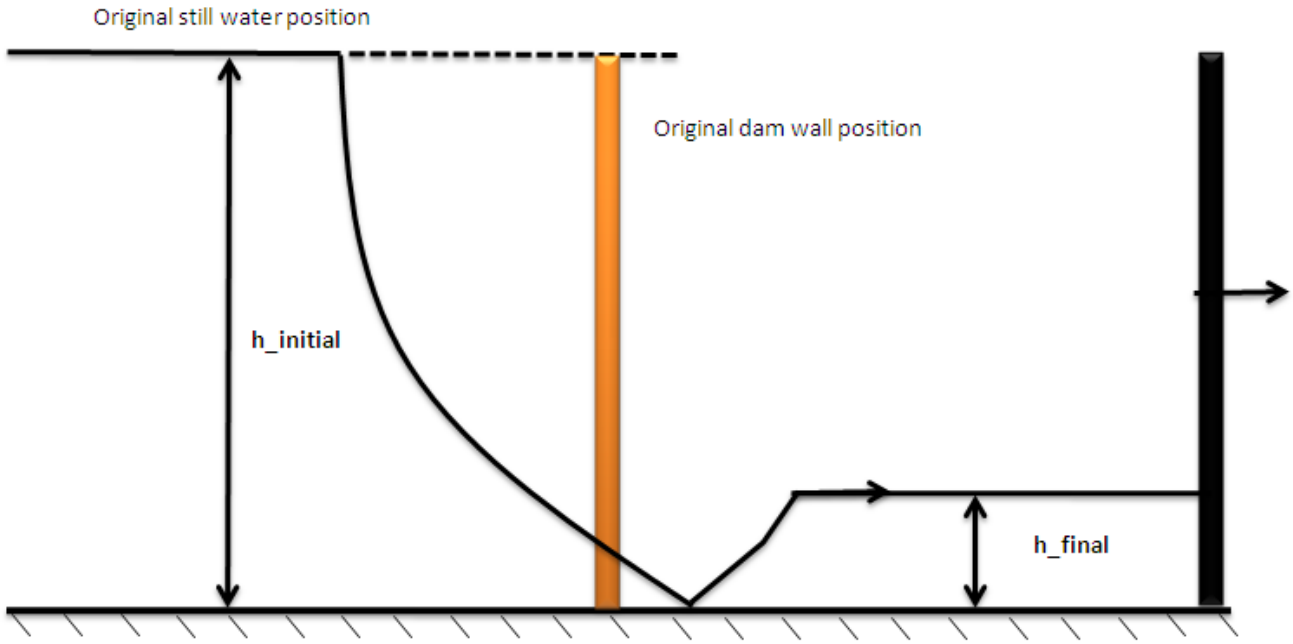

Figure 4.2: physical plane at time t

Negative Surge Case

Consider a 50m horizontal channel in which water stays at rest with constant depth $h(x,t) = 1.50m$. At the boundary $x = 0$, the following function is given in terms of the flow depth, h.

$$h(x=0,t) = \begin{cases} 1.50 & t \leq 0; \\ 1.00 & t > 0 \end{cases} \tag{4.1}$$

The experiment is done for 35 seconds within which the the spatial and duration nodes are stretched on a numerical grid of 250 equal nodes. The value of the weighted parameter for this experiment was $\theta = 0.75$ and the Froude Number of initial flow was $F_o = 0.549$.

The condition is applied across all the models and the results of the simulation are

shown in Fig. 4.3 and Fig. 4.4. From the top of Fig 4.3 is the SVE and the down subfigure is the BEM. Fig. 4.4 has the top subfigure as the KWM and the proposed model is at the down subfigure on page 56.

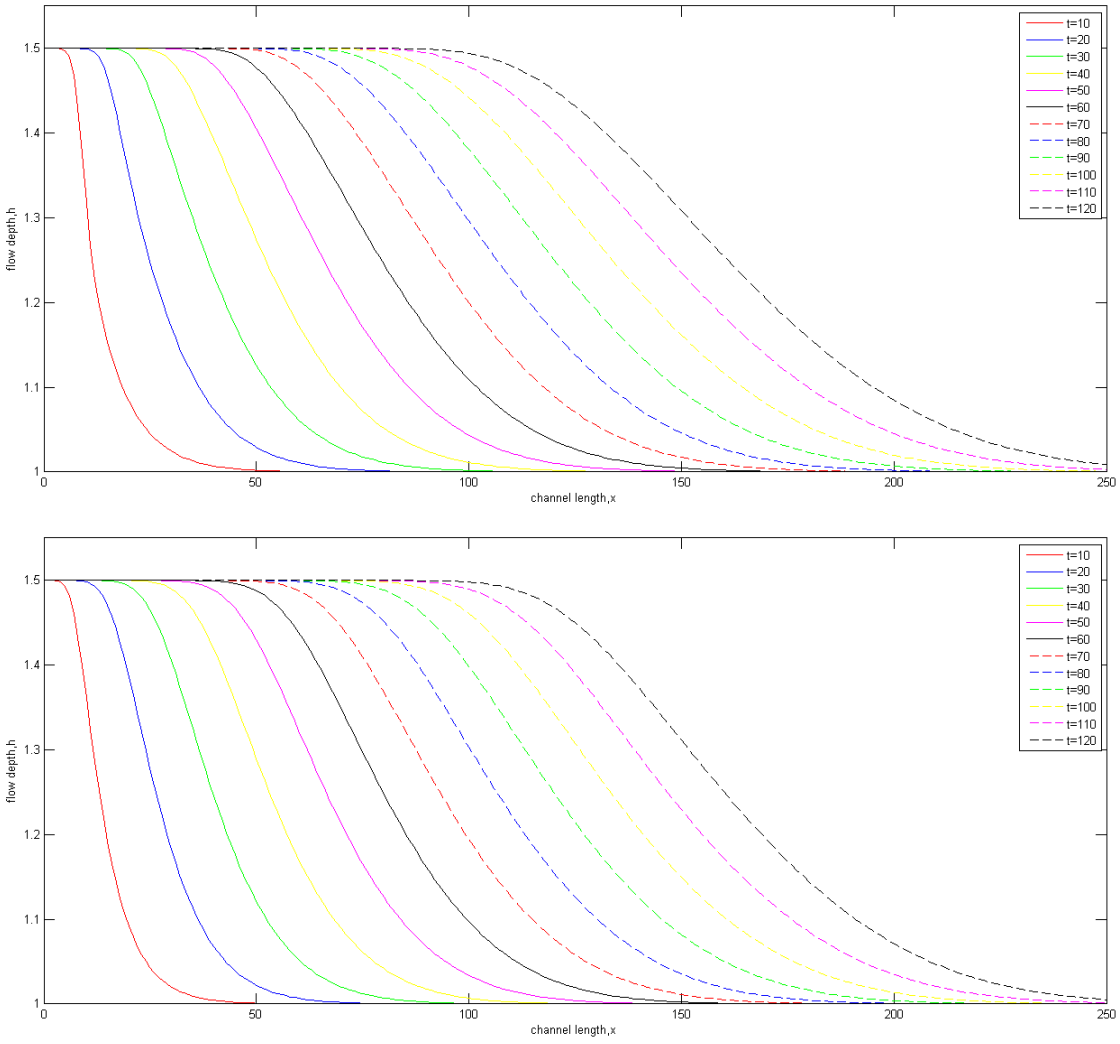

Figure 4.3: The SVE and the BEM respectively

The hydrographs displayed in Fig 4.3 show distance (x) in the horizontal axis and the predicted flow depth, h on the vertical axis with varying time, t in 10 equal intervals from

$t = 10$ to $t = 120$ units represented by the different colored straight and dotted lines.

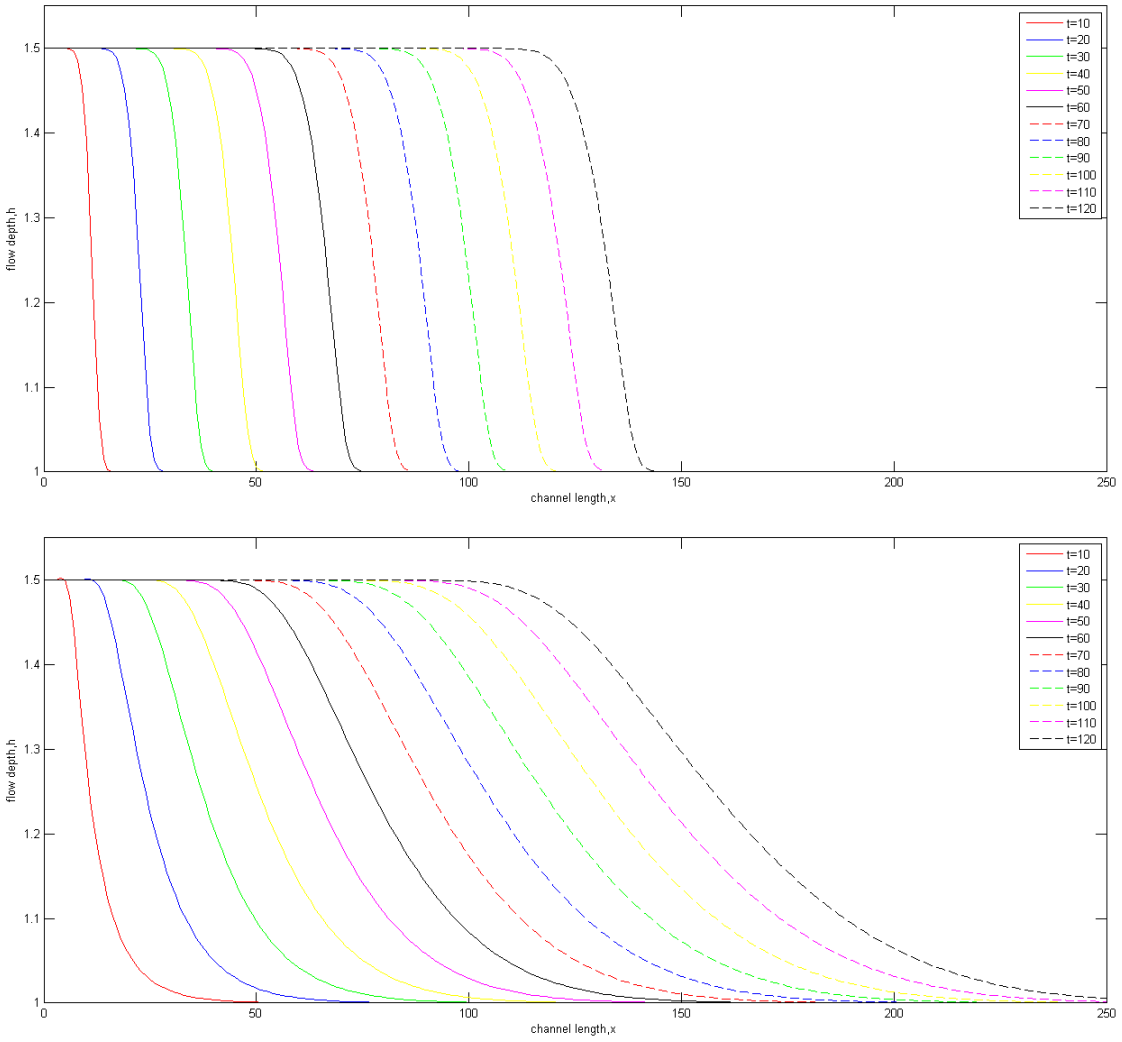

Figure 4.4: The KWM and the third approximate model

The prediction of the SVE in Fig. 4.3 of the propagation through the channel shows smooth diffused waves. The BEM for the same problem of initial flow depth of 1.5m and final depth of 1.0m shows a generally close shape to the SVE with the same pattern of diffusion. The nature of the presented third apprximate model to the SVE is very similar

to the propagation displayed by the BEM. Of the four models, the KWM displays evident less diffused waves as expected because of the absence of the diffusive term in the model that is present in the three other models (i.e. the SVE, BEM and the third approximate model to the SVE).

The BEM solution produces less steeper waves compared to the SVE with mean flow depth averagely 0.7% short of the output from the SVE. The KWM produces evidently steeper waves compared with both the SVE and BEM. The average flow depth throughout is very small (averagely 2.7% short of the SVE and 2.5% of the BEM).

4.2 Effect of Weighted Parameter

A number of experiments were carried out to determine the general effect of the weighted parameter θ in the Preissmann scheme used in discretizing the models. The results are presented in Fig 4.5, Fig. 4.6 and Fig. 4.7 for the SVE, BEM and KWM respectively. The values of θ were varied as $\theta = 0.5$, $\theta = 0.65$ and $\theta = 1.00$.

The results shows that as the weighted parameter increased, there is a general corresponding increasing diffusive effect in the solution presented by all the models. The SVE in Fig. 4.5 on page 58 for $\theta = 0.5$ shows some level of distortions along the waves produced representing the individual times especially at the initial flow depths and the final flow depths. For the other weights greater than 0.5 ($0.5 < \theta \geq 1$), the distortions disappear and there is the occurrence of smooth waves. The BEM in Fig. 4.6 page 59 shows smooth diffused waves which are more diffused as θ increases.

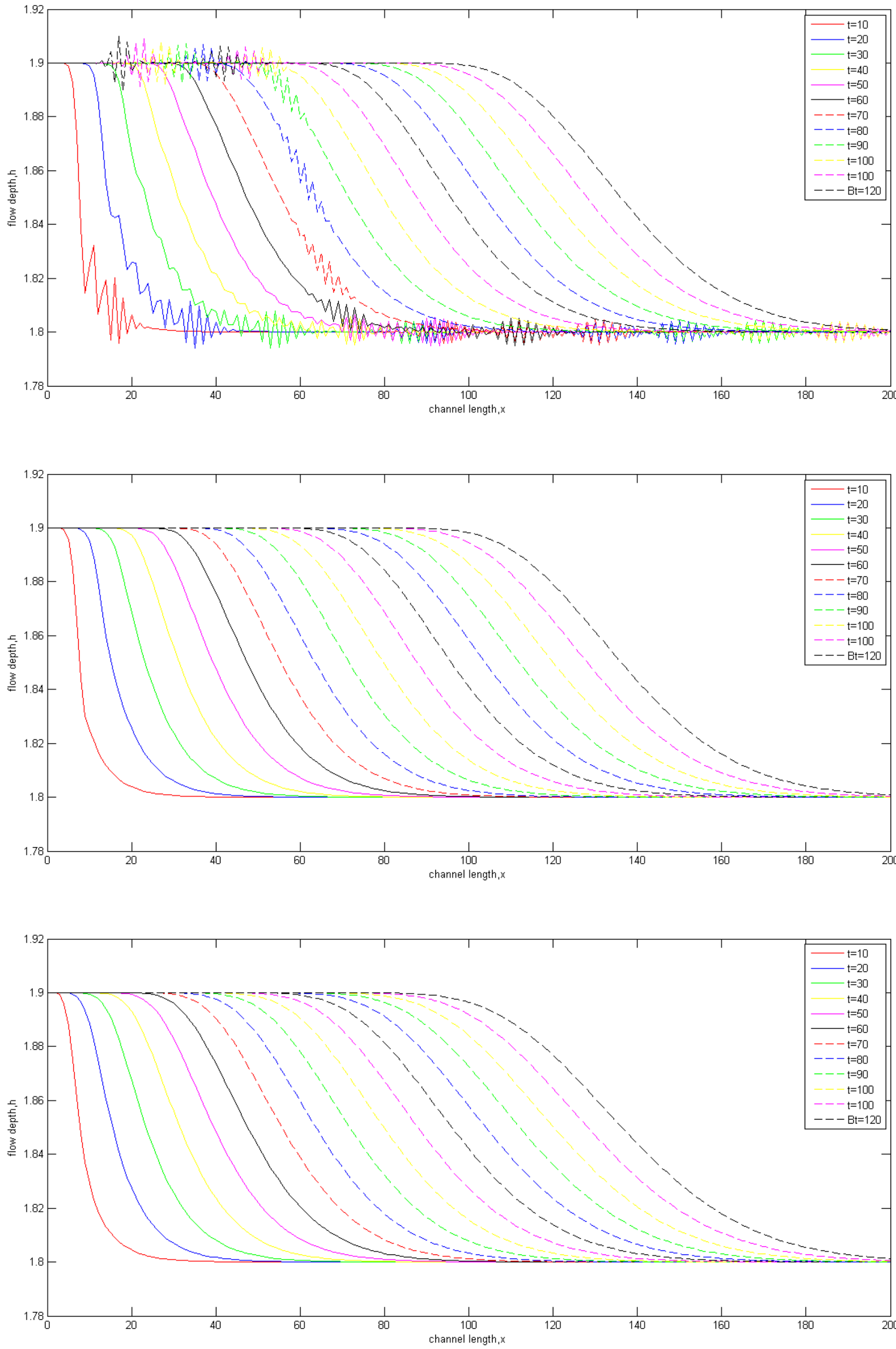

Figure 4.5: $\theta = 0.5$, $\theta = 0.65$ and $\theta = 1.00$ respectively for SVE

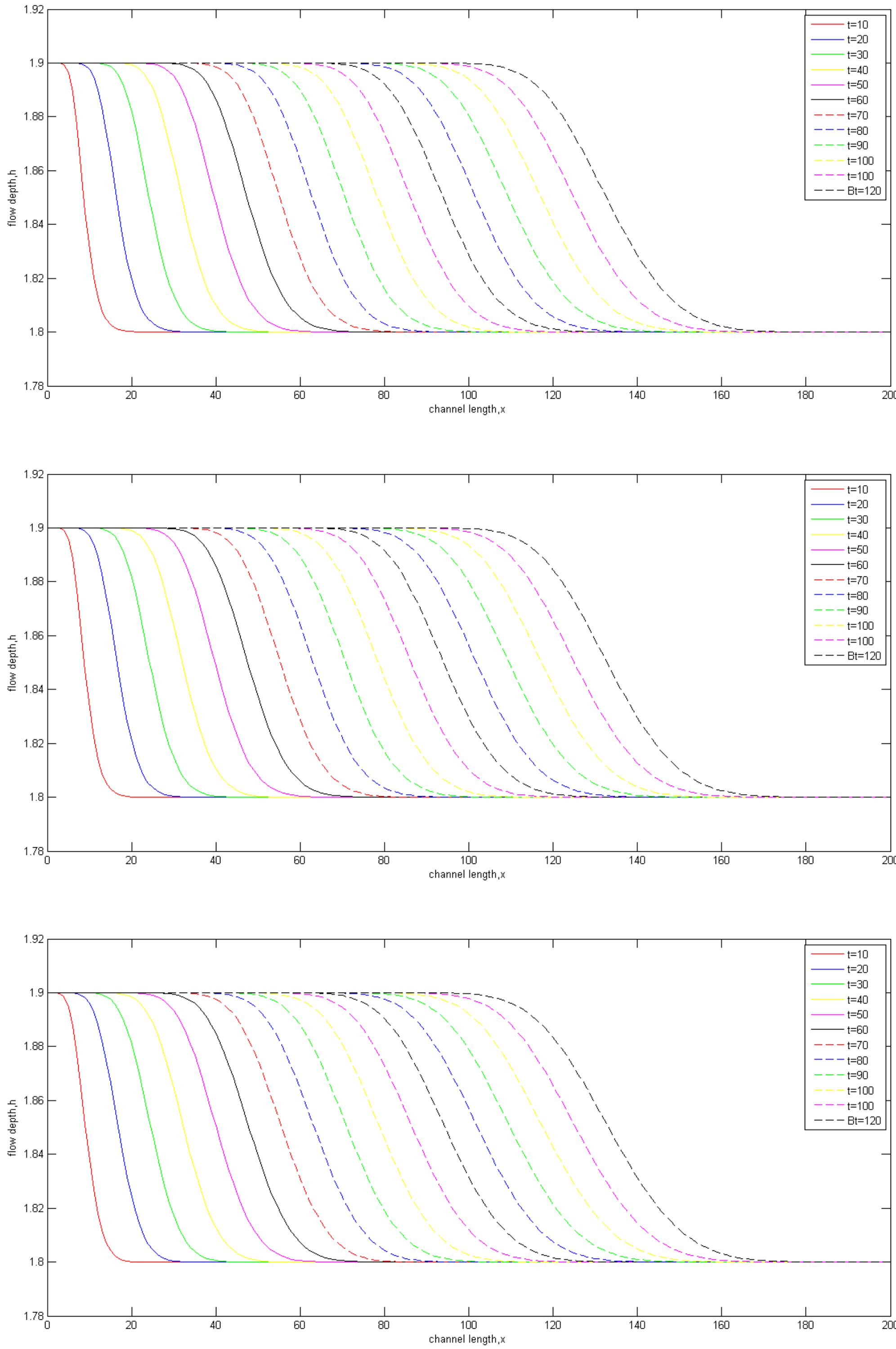

Figure 4.6: $\theta = 0.5$, $\theta = 0.65$ and $\theta = 1.00$ respectively for BEM

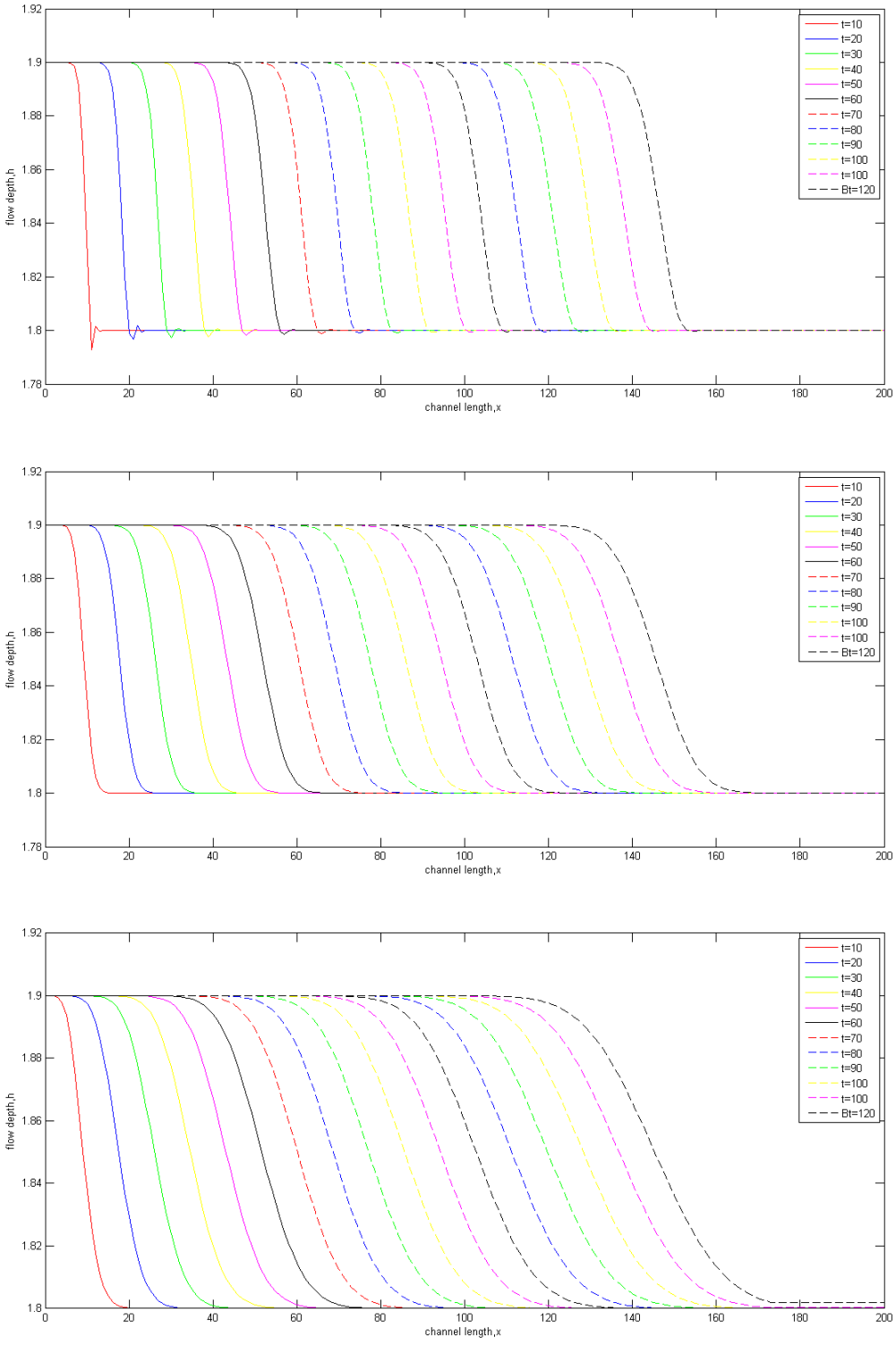

Figure 4.7: $\theta = 0.5$, $\theta = 0.65$ and $\theta = 1.00$ respectively for KWM

Mean $(h_1 - h_0)$	SVE	BEM	KWM	New Model
0.1	6.209053	0.447079	0.390647	0.457752
0.2	6.250272	0.468406	0.378322	0.469059
0.3	6.347221	0.447802	0.37436	0.463257
0.5	6.389163	0.447907	0.382700	0.458149
0.8	6.501417	0.454828	0.378633	0.460398
1.2	6.737718	0.454211	0.394196	0.459429
1.5	6.787165	0.459494	0.363316	0.466864
2.0	7.209245	0.454090	0.361972	0.495859

Table 4.1: Runtime in seconds of the SVE, BEM, KWM and the third order model

The same pattern is given off in the steep-natured solutions by the KWM. These steep waves in Fig. 4.7 on page 60 becomes slightly diffused for increasing values of the weighted parameter.

4.2.1 Runtime and Limits of Flow Depth differences

Table 4.1 on page 61 is the summary of the experiment of determining the runtime (measured in seconds) for the simulation of the hydraulic models for different mean heights. The runtime is recorded in seconds it takes Matlab to simulate the models.

For each mean difference in height $(h_1 - h_0)$, 15 different experiments were considered. Therefore the runtime for the difference in flow depth 0.1 for the SVE in Table 4.1 on page

61 given as 6.209053 seconds represents the average for 15 different flow depth difference of 0.1.

This investigation was conducted using a uniform grid of dimension 140×140 for the spatial and duration domains. The researcher observed that for every 100 node increment, the runtime for the SVE increased by averagely 364%, the runtime for the BEM increased by averagely 125% and the runtime for the KWM also increase by 206%. The presented third order approximate model to the SVE also has a runtime increment of averagely 112 % for every 100 node increment. There is a general increment in the runtime for the SVE and the KWM as the difference in between the initial flow depth and final flow depth increases. This observation is not so evident in the case of the BEM and the presented third order approximate model of the SVE.

4.2.2 Limits of the Flow Depth Differences

As one of the specific objectives of this thesis, the research seeks to determine the limits (minimum and maximum) range of the flow depth difference (between the final flow depth, h_0 and the initial flow depth, h_1) for which the parent model together with its approximate models provide acceptable results. This is done by first considering how small(minimum) the flow depth difference $(h_1 - h_0)$ can be in order for acceptable results to be obtained and then how large(maximum) difference between the initial and final flow depth can be in order to obtain acceptable results for the independent models.

The SVE when simulated with a final flow depth of $h = 1.0m$ has a minimum range of

up to $h = 1.06m$ and a maximum range of up to $h = 3.97m$ within which acceptable results are attainable. Any specified value outside this range results in unacceptable values for the simulation. When the SVE is simulated with a final flow depth of $h = 2.0m$ however, there is a minimum range of $h = 2.009m$ and a maximum range of up to $h = 7.3m$ within which acceptable results are given. A simulation of the SVE with a final flow depth of $h = 5.0m$ has a minimum of $h = 5.01$ and a maximum range of up to $h = 16.2m$. For values higher than $h = 5.0m$ however, there is a similar trend of the minimum range within 2% of the specified flow depth and a maximum of up to 3 times the specified flow depth.

Interestingly noted was the fact that there seemed to be no maximum range for which the KWM can be simulated. The results as the range is increased is a melon-like structure as shown in Fig. 4.8.

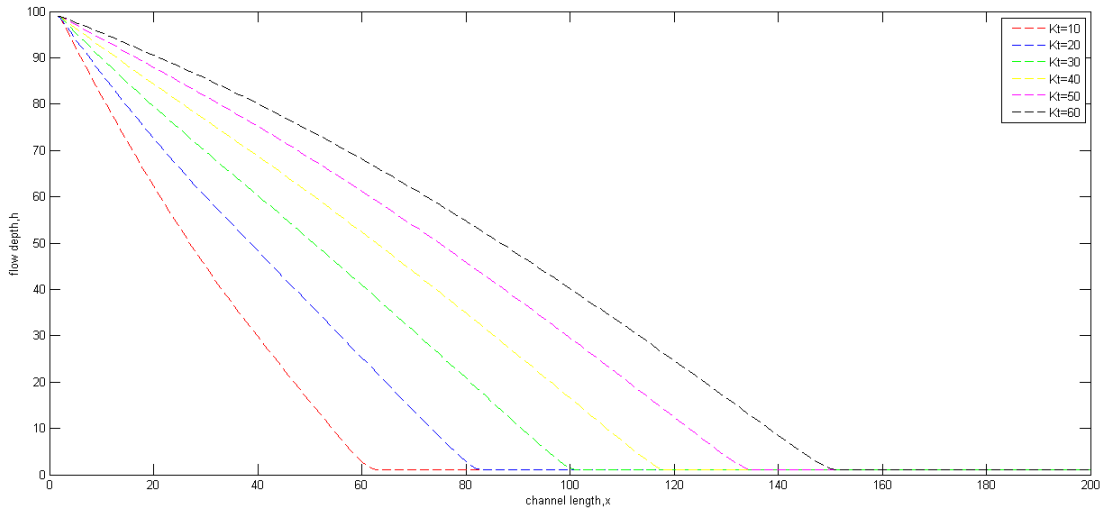

Figure 4.8: Simulation of KWM with extremely high flow depth differences

The Kinematic Wave equation when simulated using the final flow depth of $h = 1.0m$

has the minimum range of up to $h = 1.06$ for the generation of acceptable results. Similarly, when simulated using a final flow depth of $h = 2.0m$ and $h = 5.0m$, the minimum range results of up to $h = 2.06$ and $h = 5.09m$ respectively for acceptable results.

The BEM and the third order approximate model to the SVE also deliver acceptable results irrespective of extremely small minimum values, for example specifying a final flow depth of $h = 1.0m$ results in a minimum of as low as $h = 1.00000000009m$ for which acceptable results are generated for any specified value within. This holds for the BEM and the third order approximate model to the SVE.

4.3 Quantitative Comparison

This subsection provides experiments on the point by point prediction of the approximate models (The KWM, the BEM and the presented third order approximate model to the SVE) in comparison to the Saint Venant equations (SVE). There is the use of graphical techniques for comparison supported with relative percentage errors that measure the deviations of the solutions of the considered approximate models to the SVE.

The BEM is compared to the SVE and the KWM is also compared to the SVE by examining exactly the quantum of errors generated by using these models in place of the SVE. The BEM is then placed on the same grid with the third order approximate model. Finally, all the approximate models are compared to the parent model, the SVE by first considering the BEM with the third order approximate model and then the BEM along with the KWM also on the same scale.

4.3.1 The SVE and the BEM

The figure below (Fig 4.9) shows the hydrograph for the SVE (— straight line) and the BEM (- - - dashes) on a 250×250 grid structure for an initial flow depth of $h = 1.5m$ and a final flow depth of $h = 1.0m$.

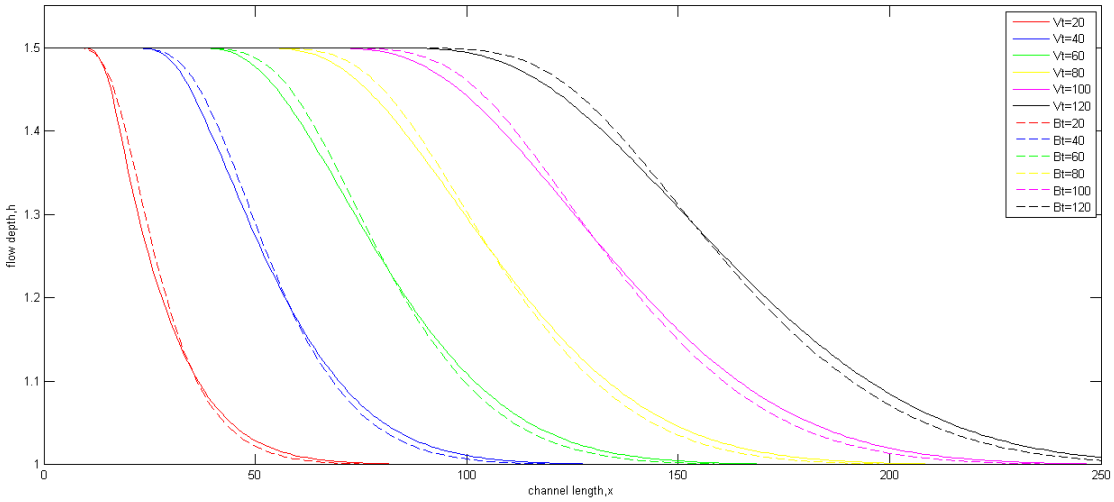

Figure 4.9: Distance-time graph for SVE versus BEM

Fig 4.9 shows that the BEM simulates well the results shown by the SVE. It results in producing almost an exact mimic to the SVE. At $t = 20$, the prediction of the BEM is 0.1% lower than the SVE between a mean distance of about 15m. It then predicts exactly as the SVE and then starts to overpredict after about $15m$.

At $t = 20$ and beyond however, the BEM starts with over predicting the SVE estimates as low as 0.09% and then predicts exactly as SVE along the channel for a mean distance of 5.0m and then overpredicts the SVE after that. This overprediction spans till the end of the channel. The minimum percentage underprediction of the BEM throughout the channel

is 1.5%. The maximum pecentage overprediction is 2.9%. To demonstrate the consistent nature of the errors generated the another problem of grid structure 200×200 is simulated. The percentage errors given throughout the channel for time steps of 20 units is given in Fig 4.10 for the specified simulation.

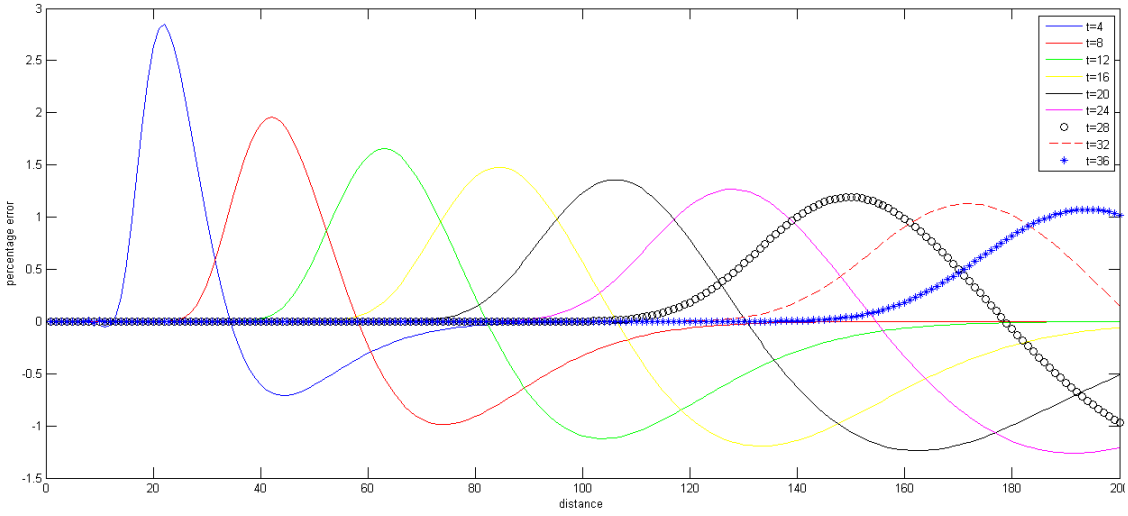

Figure 4.10: Distance-time percentage error plot for the SVE and the BEM

4.3.2 The KWM and the SVE

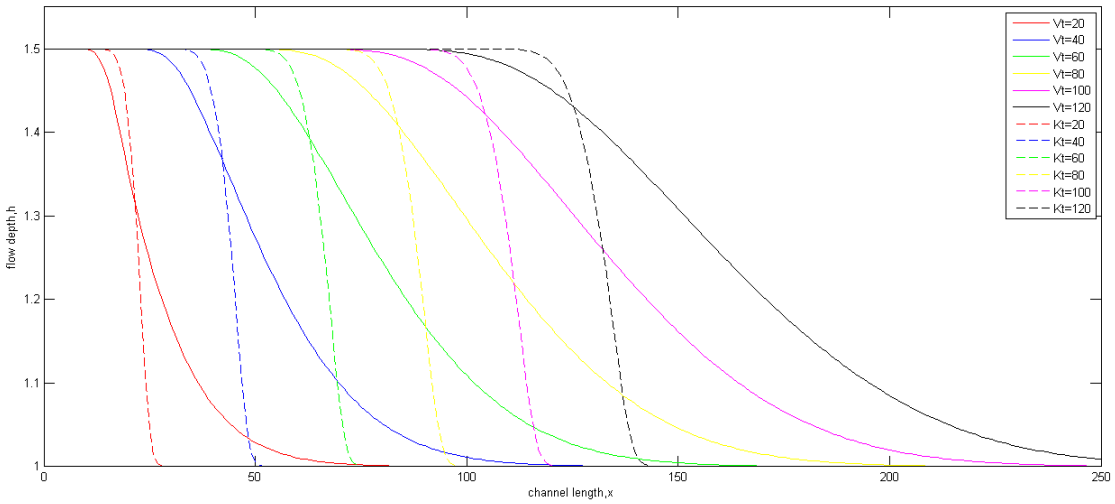

Figure 4.11: Distance-time graph for SVE versus KWM

Fig. 4.11 is the 2-D plot of the KWM and the SVE propagation prediction throughout the channel for selected time values. It starts from $t = 20$ to $t = 120$. The way the KWM predicts propagation is very different from the BEM. It constantly over predicts from the start of the channel after the dam breaks and then equals the SVE for a relatively short distance of 2m. For most time calculations, however the intervals for which the predictions of the KWM equal the SVE are points along the channel after which which it under predicts the SVE. The minimum over prediction given by the KWM relative to the SVE is 5.0 % whiles the maximum over prediction is up to 30%.

Fig. 4.12 on page 68 is a percentage-distance plot indicating the errors of the KWM relative to the SVE. This indicates the high quantum by which the KWM under predicts the SVE.

For the purposes of consistency, a different structure is considered being 200×200. Fig 4.12 is therefore the results for the relative percentage errors generated for the problem of initial flow depth being $h = 1.5m$ and a final flow depth of $h = 1.0m$

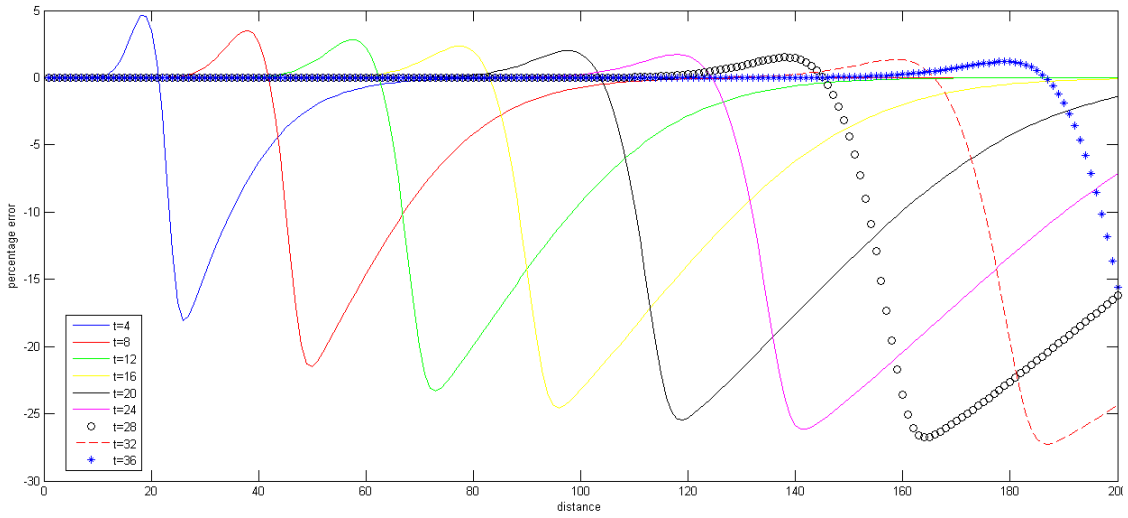

Figure 4.12: Distance-time percentage error plot for the SVE and the BEM

4.3.3 The Third Order Approximate Model and the SVE

The figure below (Fig 4.913) shows the hydrograph for the SVE (— straight line) and the third order approximate model to the SVE (- - - dashes) on a 250×250 grid structure for an initial flow depth of $h = 1.5m$ and a final flow depth of $h = 1.0m$. This look very similar to the simulation of the BEM.

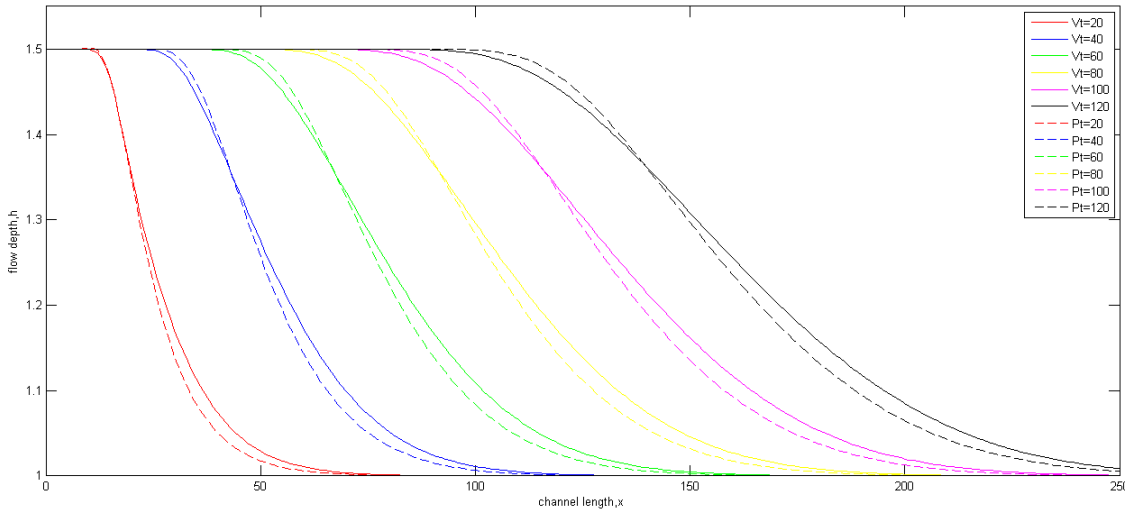

Figure 4.13: Distance-time graph for the SVE and the third order model

The relative percentage errors demonstrate the difference between the third order approximate model to the SVE and the results obtained from the BEM. Fig 4.14 on page 70 shows that the maximum over prediction tapper just around 1% with the maximum relative percentage deviation almost 2.5%. Fig. 4.14 is 200×200 grid scale demonstration of the relative percentage error comparison of the third order approximate model to the SVE.

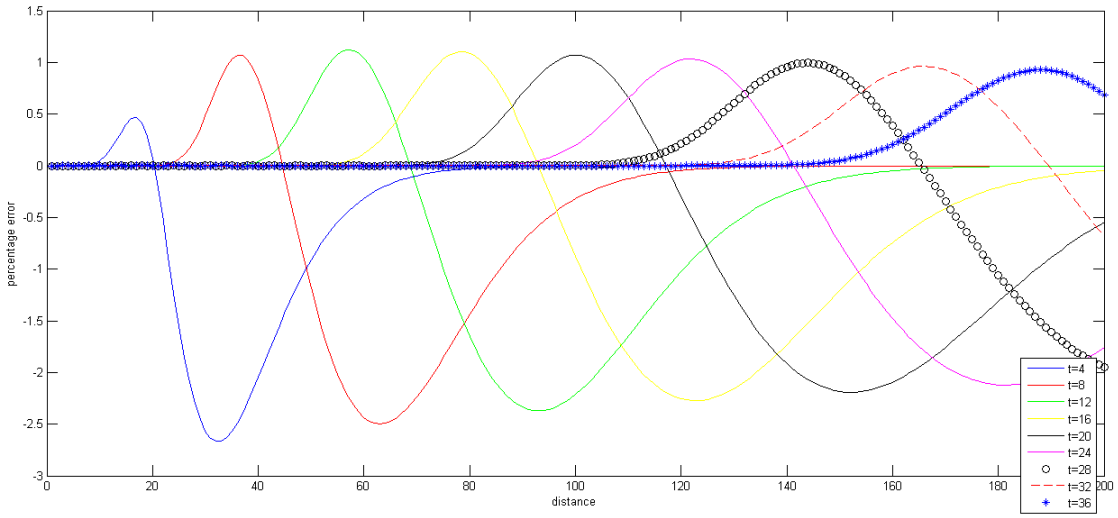

Figure 4.14: Percentage errors for the third approximate model to the SVE

4.3.4 The BEM and the Proposed Approximate Model

Fig. 4.15 shows the comparative hydrograph of the simulation by the BEM and the third order approximate model on the same grid. The effect of the third order derivative addition shows a smooth slight over prediction by the third order model away from the initial flow depth $h = 1.5m$. When the flow depth averages $h = 1.474m$, the two models (The BEM and the third order approximate model) present exactly the same solution for varying intervals. This pattern is consistent throughout the propagation. The rest of the propagation however shows that the third order derivative model under predicts what the BEM model displays. Towards the end of the channel, averagely when $h = 1.01m$, the two models predict the same results.

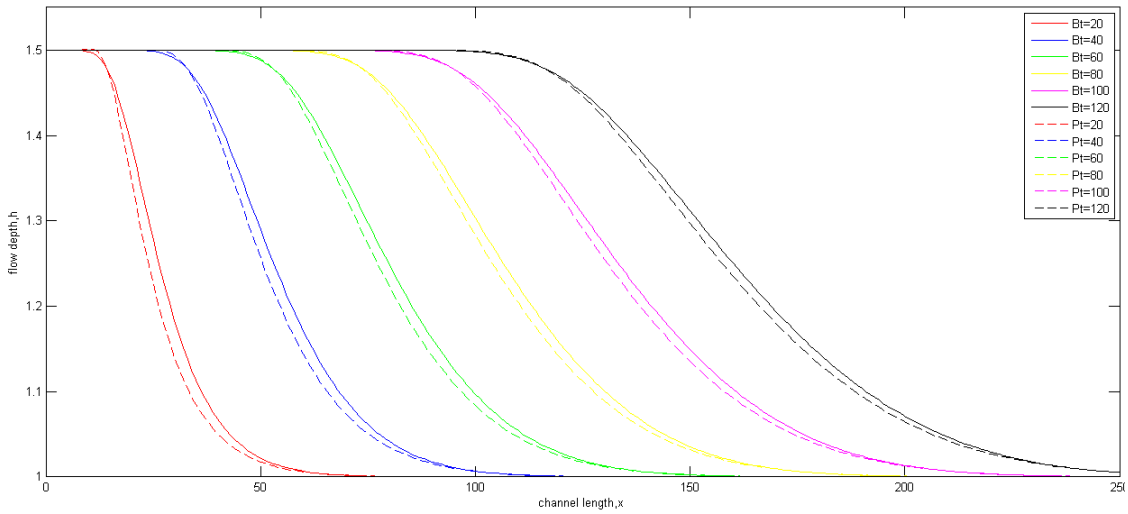

Figure 4.15: Distance-time graph for the BEM and the third order model

4.3.5 The SVE, BEM and the Proposed Approximate Model

To access how well the third order approximate model mimics the results by the SVE compared to the dominance of the BEM, the three models (the third order approximate model (- - -), the BEM (**) and the SVE(—)) are examined on the same structure. Fig 4.16 shows the hydrograph displaying a 250 node solution of water staged at an initial flow depth of $h = 1.5m$ with a final flow depth of $h = 1.0m$

From the nature of the results shown in Fig 4.16, the advantage of the third order approximate model can be established. Apart from the relative error comparison demonstrating the minimum over prediction by the third order model, it is also observed that the two approximate models equal the SVE at different points along the propagation. The BEM solution equals the SVE at averagely $h = 1.37m$. The presented third order model on the other hand equals the SVE at past midway averagely when the flow depth, $h = 1.19m$

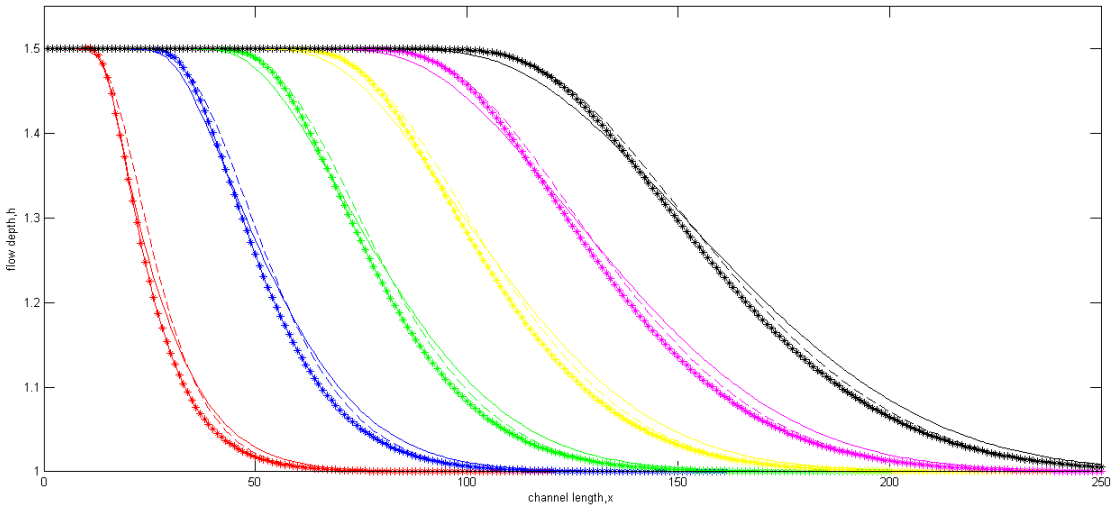

Figure 4.16: Distance-time SVE, BEM and third order model

The comparison of the SVE, BEM and KWM show similar patterns by the fact that the approximate model equals the parent model at different points. The plot of the three models for the same problem is given in Fig. 15.

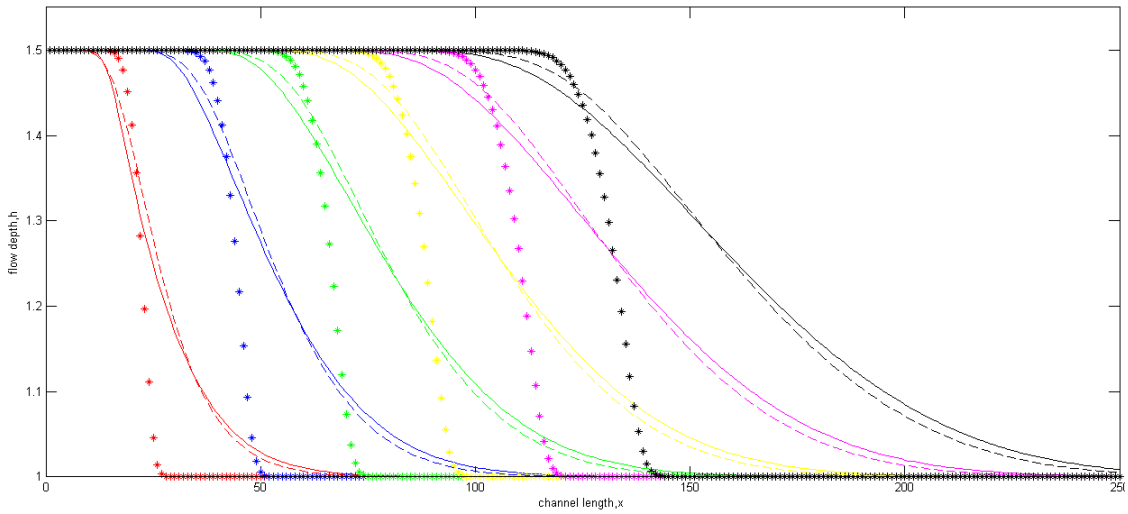

Figure 4.17: Distance-time SVE, BEM and KWM

4.4 Positive Surge

A positive surge results from a sudden change in flow that increases the depth. It is an abrupt wave front. The unsteady flow conditions may be solved as a quasi-steady flow situation (Chanson (2004)).

This can result when a dam breaks from the downstream point. The wave therefore rises from the lower initial point and steadily rises to a higher final flow depth.

Consider a channel that has water stage and is released at an initial constant depth $h(x,t) = 1.0m$. At the boundary $x = 0$, the following function is given in terms of the flow depth, h.

The dynamics of the SVE, BEM and KWM are given in Fig. 4.18 respectively.

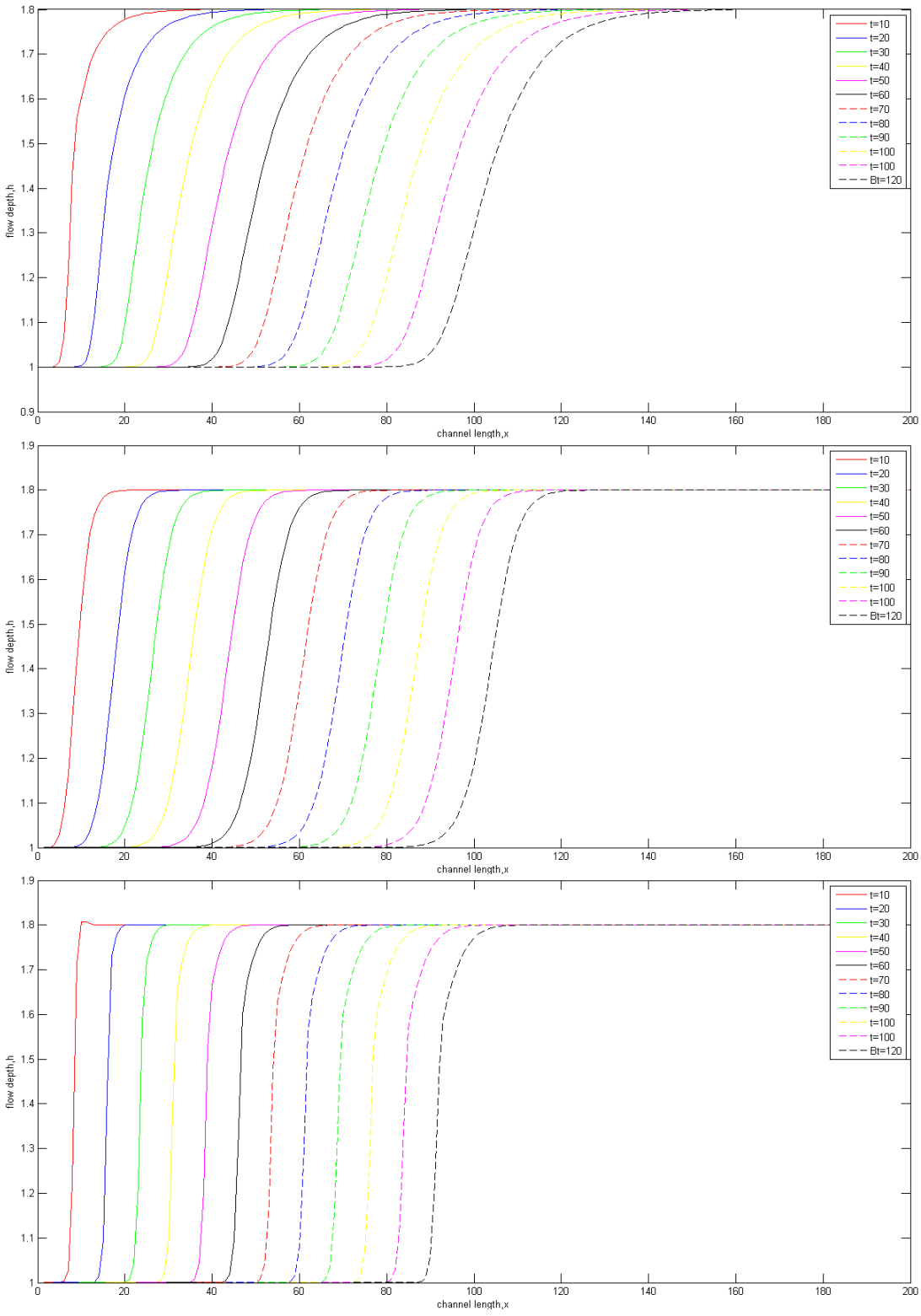

Figure 4.18: Increasing time nodes $t_{10} \Rightarrow t_n$ for SVE, BEM and KWM respectively

4.5 Efficiency Criteria

The efficiency criteria for hydraulic models discussed in Chapter 3 is evluated for the models. Since there is a comparison of the two approximate models against the SVE, the observed values O_i are the values of the output from the SVE for any given simulation while the predicted value, P_i are those of either the BEM, the third order model or the KWM.

4.5.0.1 The BEM and SVE

A channel of length 50 discretized into 200 equal nodes is considered. The solution for the dynamics of the flow depth is therefore in a matrix of dimension 200×200. The progression of the prediction by the BEM is considered first relative to the SVE. The plots of the various efficiency criteria is calculated from the initial point to half the channel (i.e. $t = 0 - t = 100$), then from ($t = 0 - t = 150$),from $t = 0 - t = 170$) and then from for the overall channel is considered ($t = 0 - t = 200$).

Fig. 4.19 and 4.20 are two dimensional graphs that represent the same progression of a wave within a channel of length 50m discretized into 200 nodes. The graphs are presented in 2×2 array. In explaining, we make use of the notation f_{ij} to mean the ith row graph and the jth column graph.

As seen in f_{11} and f_{12}, Fig 4.19 shows the same progression from the initial point to halfway the channel for the different discussed efficiency criteria. The prediction by the BEM is a bit distorted for almost all criteria up to $t = 10$.

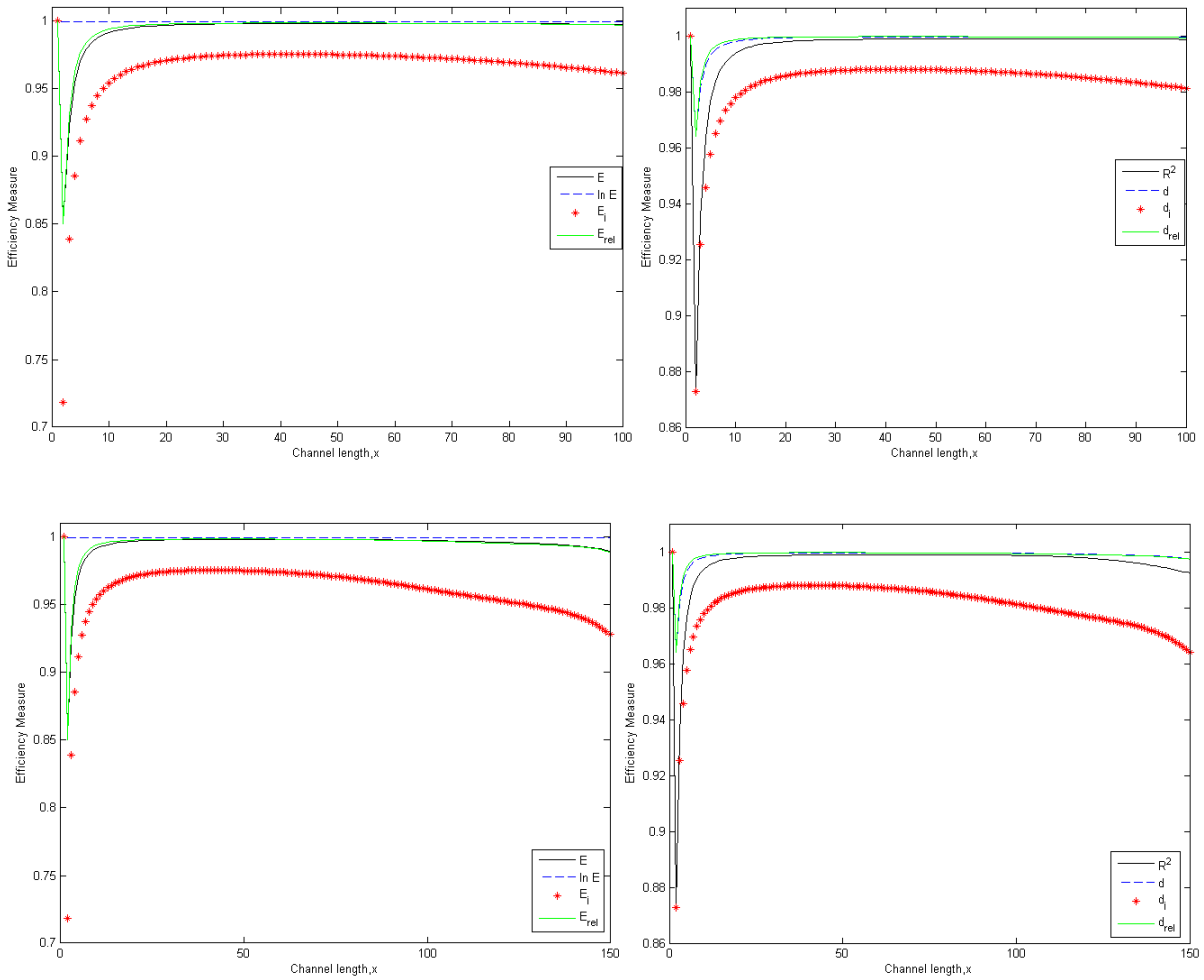

Figure 4.19: Efficiency Criteria for the prediction by BEM

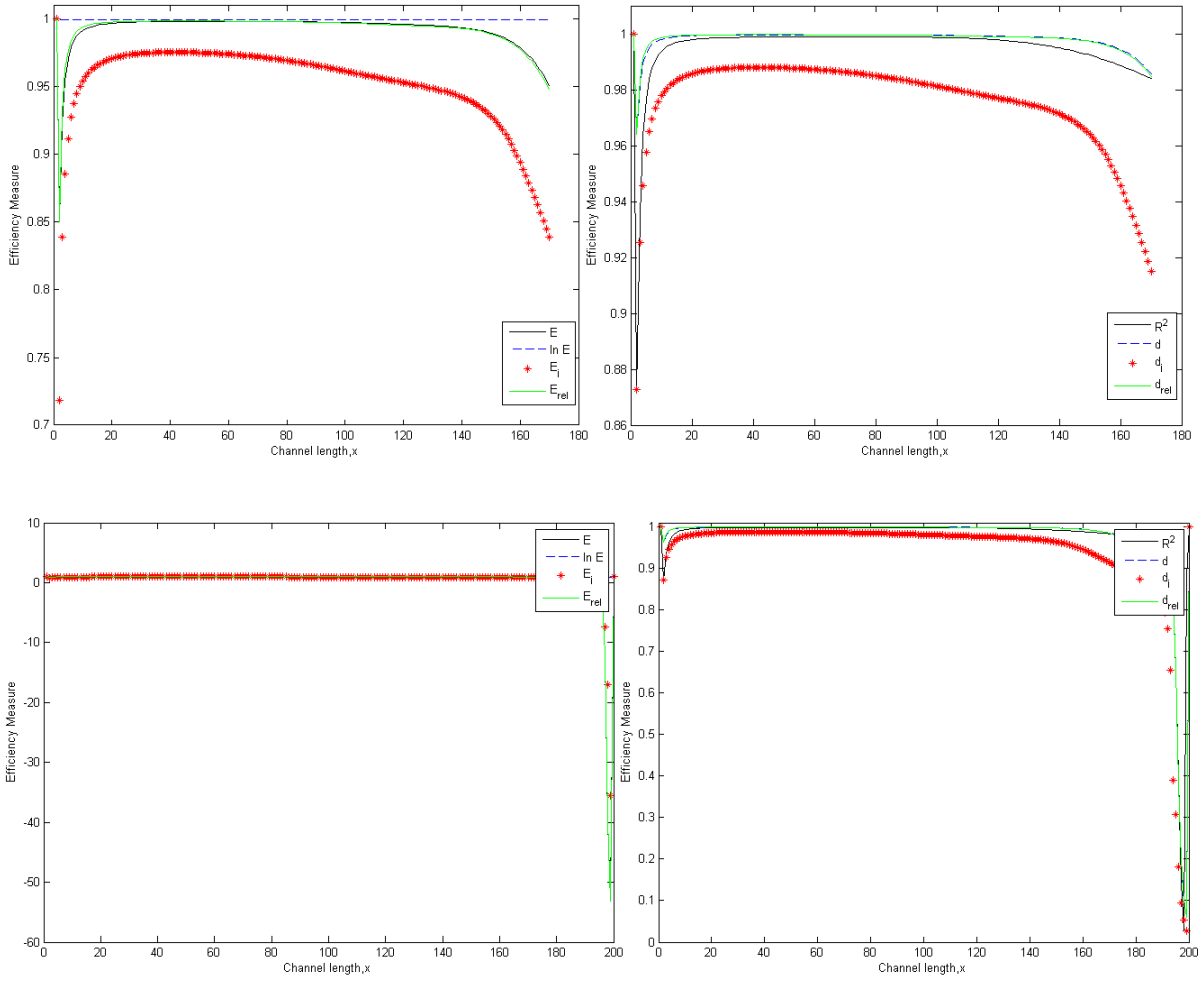

Figure 4.20: Efficiency Criteria for the prediction by BEM

After $t = 10$ however, the prediction is stable, averagely 0.99 for all criteria till halfway the channel. $r^2 = 0.9989$, $E = 0.9985$,$d = 1.000$, $\ln E = 0.999$, $E_j = 0.9605$,$d_j = 0.9649$, $E_{rel} = 0.9942$ and $d_{rel} = 0.9979$.

f_{21} and f_{22} from Fig 4.19 displays the prediction from the initial up to $t = 150$. It is observed that the models starts to under predict will all measures starting to drop except for $\ln E$ which remains close to 1.

After $t = 150$, there is a massive change in all measures including $\ln E$ with d_j responding very sensitively to the difference in SVE and BEM values. Towards the end of the channel, the coefficient records low fit between the SVE and BEM. (i.e. $r^2 = 0.0278$ with $E = -39.87$ and $d_j = 0.0526$). This is shown in Fig 4.20.

4.5.0.2 The KWM and SVE

The efficiency criteria is again used to investigate the predictive performance of the KWM relative to the SVE for the same problem with grid dimension of 200×200.

The graphs are constructed in progression from initial to halfway ($t = 0 - t = 200$), then from $t = 0 - t = 150$, $t = 0 - t = 170$ and then from $t = 0 - t = 200$.

f_{21} and f_{22} of Fig 4.21 displays ($t = 0 - t = 100$). There is a general decline in the measures except for $\ln E$ which remains equal to 1. There is however almost no distortion to initial from from $t = 0 - t = 10$. The prediction gives a range or 0.9-0.5 averagely for the efficiency measures. f_{11} and f_{12} of Fig 4.22 displays a general decline in the measures

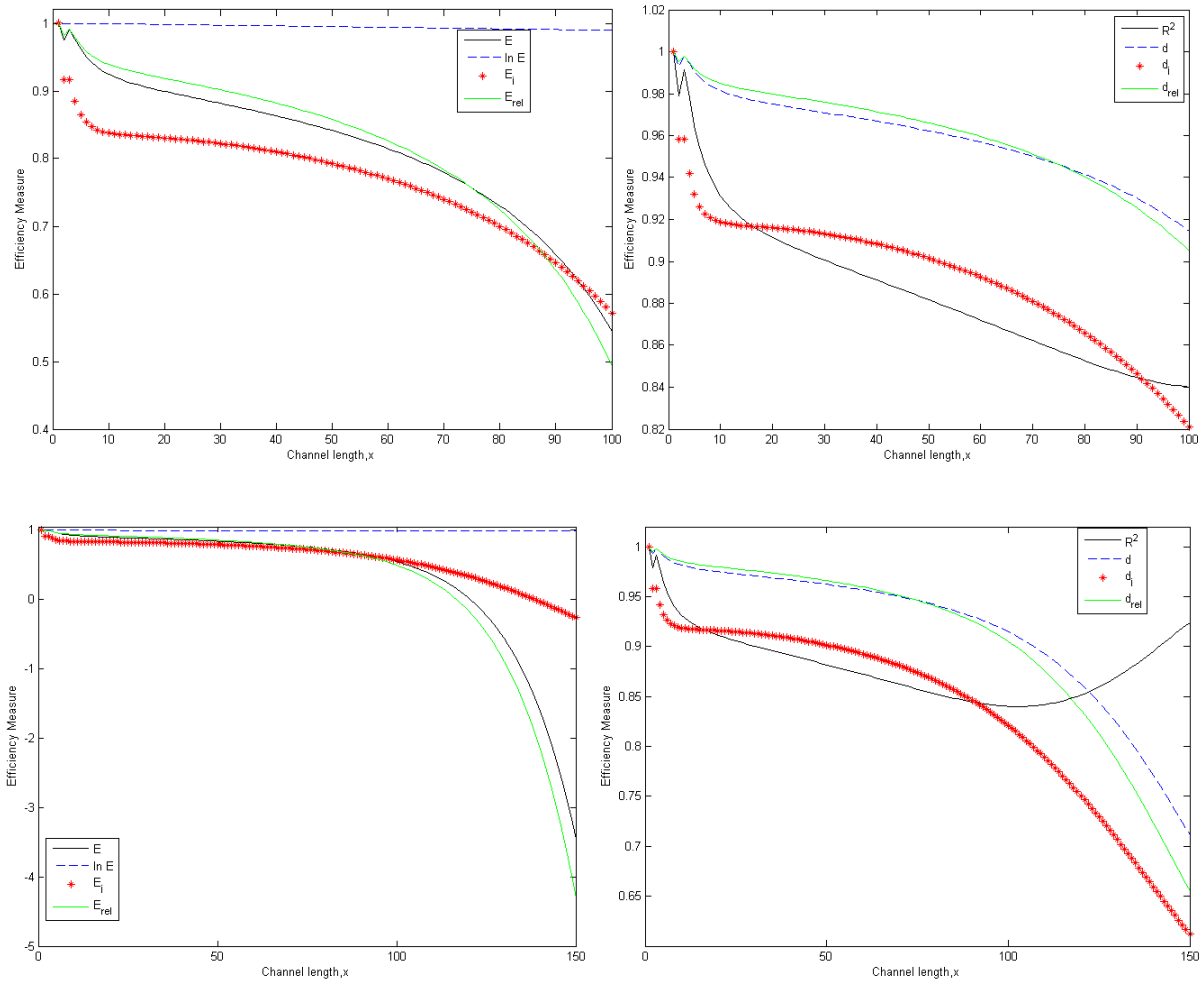

Figure 4.21: Efficiency Criteria for the prediction by KWM

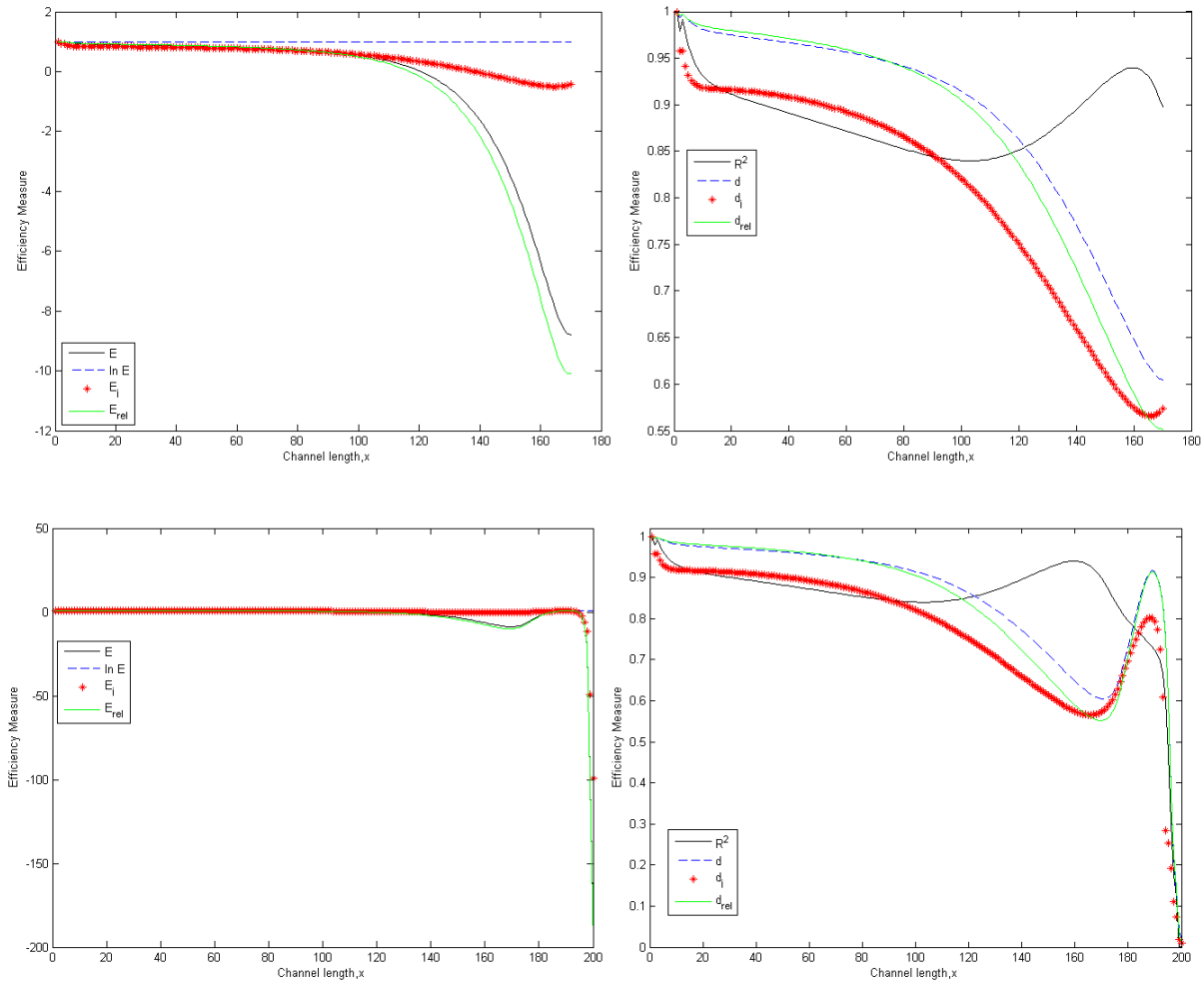

Figure 4.22: Efficiency Criteria for the prediction by KWM

but very steep. E_j and E_{rel} measures as far as -7.62 and -9.1 respectively.

f_{11} and f_{12} of Fig 4.22 shows the overall prediction of the KWM for the SVE. Towards the end of the channel specifically between $t = 195$ to $t = 200$, there are very low measures ranges as follows: $r^2 = 0.0002 - 0.30$, $E = -198.9121 - (-2.3164)$,$d = 0.0195 - 0.2212$, $\ln E = 0.83 - 0.99$, $E_j = -98.97 - (2.422)$,$d_j = 0.0099 - 0.1117$, $E_{rel} = -199.9129 - (-0.0632)$ and $d_{rel} = 0.0446 - 0.3754$.

4.5.0.3 The Third Order Model and SVE

The efficiency criteria is finally used to investigate the predictive performance of the third order approximate model relative to the SVE for the same problem with grid dimension of 200×200.

f_{11} and f_{12} of Fig 4.23 displays ($t = 0 - t = 100$). There is a large correspondence between the values here the BEM. For almost all the efficiency measures except E_rel, there is recording of between 0.9-1.0.

f_{21} and f_{22} of Fig 4.24 shows the overall prediction of the third order approximate model relative to the SVE. Towards the end of the channel specifically between $t = 196$ to $t = 200$, there are very low measures ranges as follows: $r^2 = 0.082 - 0.30$, $E = -162.9121 - (-2.3164)$,$d = 0.0385 - 0.8$, $\ln E = 0.91 - 0.99$, $E_j = -40.61 - (1.54)$,$d_j = 0.0239 - 0.1133$, $E_{rel} = -213.89 - (-0.1632)$ and $d_{rel} = 0.0556 - 0.5783$.

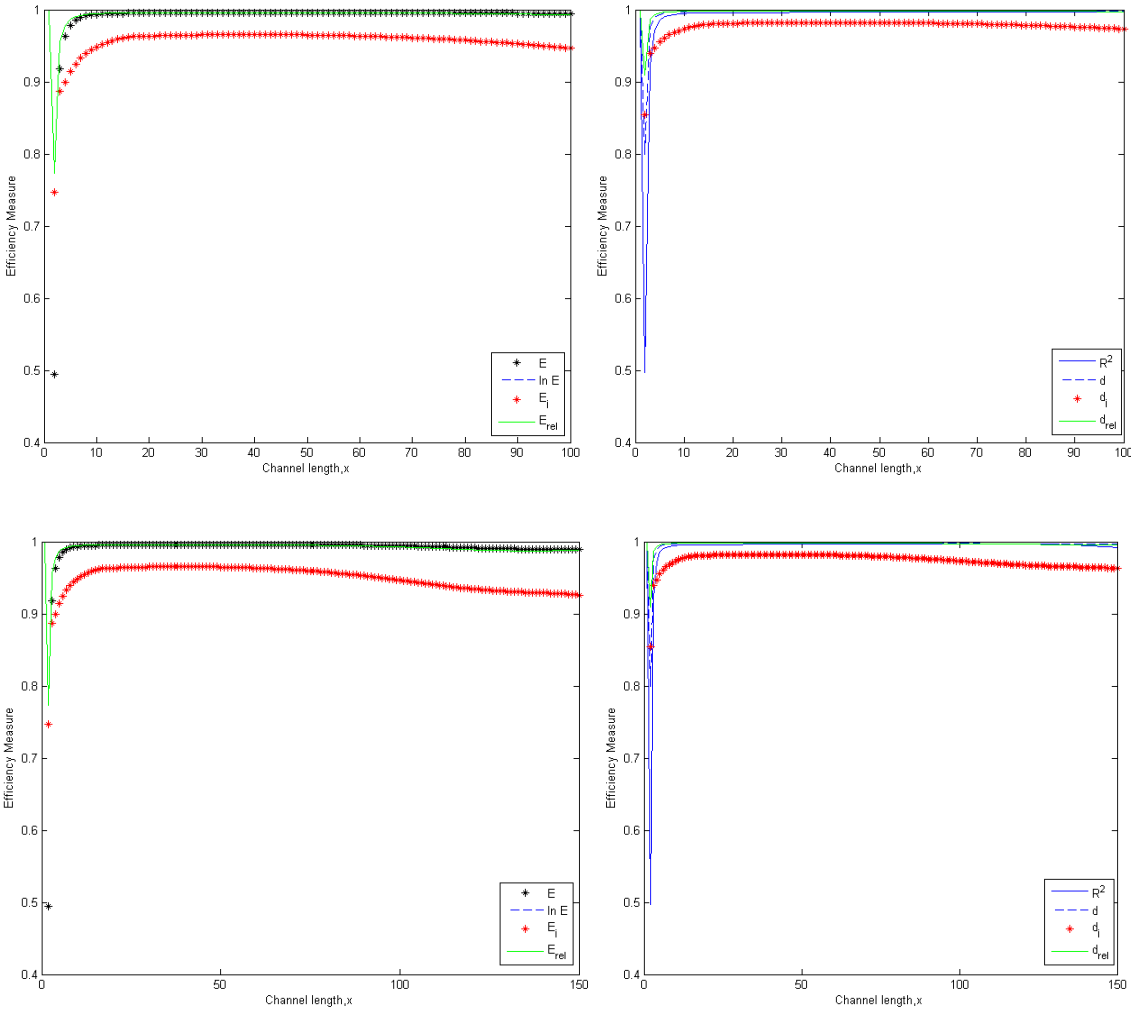

Figure 4.23: Efficiency Criteria for the prediction by the Third Order Model

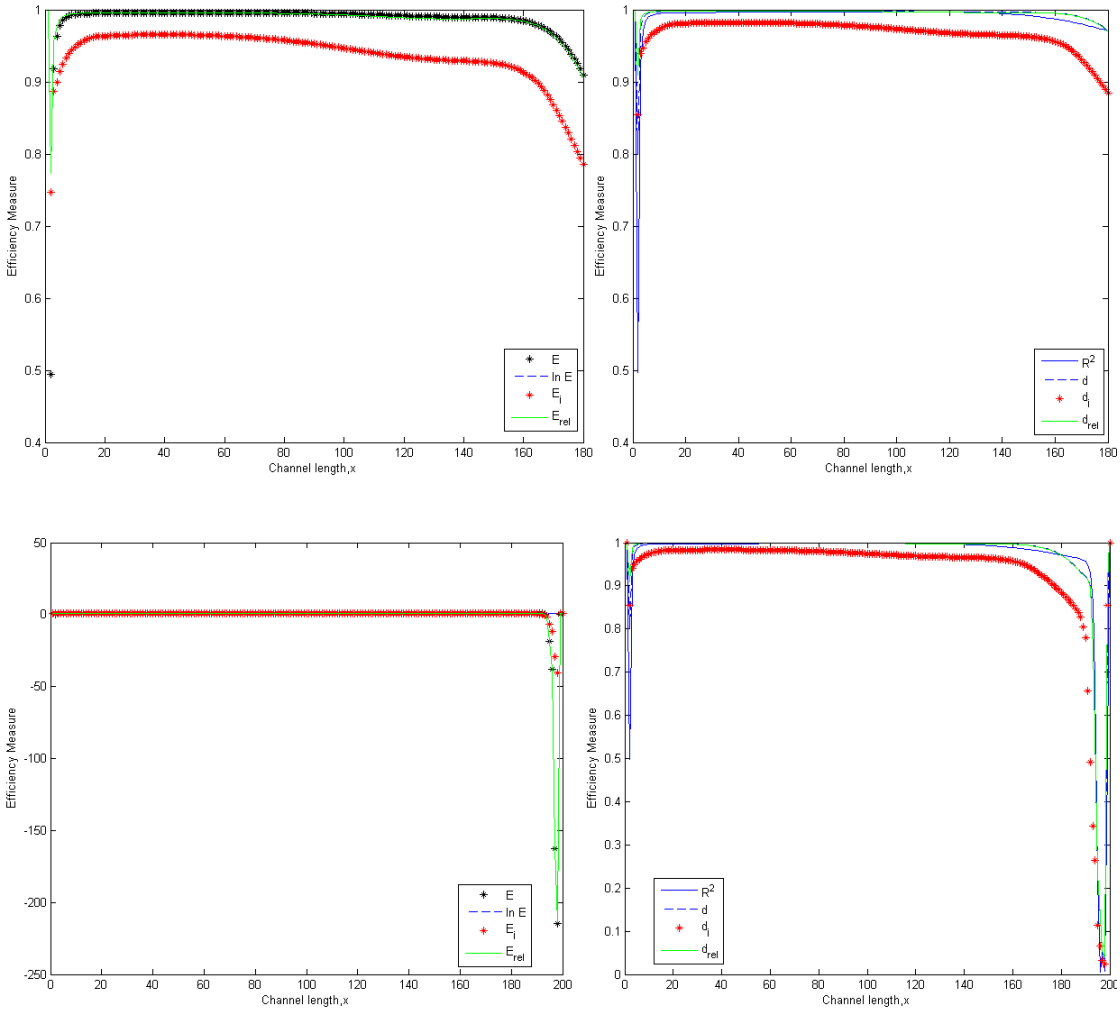

Figure 4.24: Efficiency Criteria for the prediction by the Third Oder Model

Chapter 5

Conclusion and Recommendations

5.1 Introduction

The key objectives of this research were to consider the Saint Venant Equations (SVE) and its approximate models i.e. the Burgers Equation Model (BEM) and the Kinematic Wave Equation (KWM) for which are second order and first order approximate respectively. In addition to this, a third order approximate model is proposed and presented in this thesis. The third order approximate model to the SVE and the two existent approximate models are therefore quantitatively analyzed with the inclusion of graphical techniques. The approximate models together with the parent model are solved using finite differences (specifically the Preissmann scheme).

The researcher uses MATLAB to program the algorithms to simulate the models.The quantitative analysis is performed using percentage errors and then using efficiency criteria for hydraulic models. Also considered was the range within which acceptable results are generated for all the individual models.

5.2 Conclusion

The conclusions in this research are summarized as follows:

- The estimated third order approximate model to the SVE has preserved forms of the constant coefficients of the KWM and the BEM for the first and second orders respectively
- The estimated constant of the third derivative has a magnitude of

$$\frac{F_o^2}{3}\left(1-\frac{4}{9}F_o^2\right)$$

- The third order approximate model equals the SVE at a lower level consistently compared to the BEM at a higher flow depth level
- The third order approximate model is most efficient model quantitatively taking away other advantages of the BEM
- The KWM has a minimum range of simulation but can be used to simulate problems with extremely wide flow depth differences.
- The weighted parameter within the box scheme has a positive relationship with the diffusive nature of the waves. An increment in the weighted parameter increases the diffusive nature of all the models considered in this research.
- The BEM in its given form simulates well the SVE with far less computional cost of time of as low as 3,000% less time than it takes to run one simulation for the

SVE. The result is based on implicit schemes employed to solve both equations and therefore has established an insurance of stability. The range of over prediction and under prediction for the BEM relative to the SVE is 2.34% and 1.5% respectively.

- The KWM therefore apart from it's steep wave producing form provides no advantage over the BEM relative to the SVE. The BEM with its extremely low runtime can well be used in place of the SVE.

5.3 Recommendation

The researcher recommends an investigation into the distortion that occurs at the end of the prediction by the KWM. This qualitative observation also occurs in implicit schemes for all the models considered when the problem is solved in the region of $dt > dx$.

This occurrence may account for the instantaneous movement of the dam wall in the Dam Break problem.

The third order approximate model can be used together with the BEM since they predict equal to the SVE at a lower and higher flow depth point respectively

Bibliography

Akan, A. O., & Yen, B. C. (1977). A nonlinear diffusion-wave model for unsteady open-channel flow. *Proc., 17th Congress, Int. Association for Hydraulic Research*, *2*, 181190.

Beven, J. K. (2001). Rainfall-runoff modelling. *The Primer, John Wiley and Sons Ltd, Chichester*, 319.

Burgers, J. M. (1950). Correlation problems in a one-dimensional model of turbulence. *Proc., Royal Netherlands Academy of Science, Amsterdam*, *53*, 247-260.

Chanson, H. (2004). Environmental hydraulics of open channel flows. *Elsevier Butterworth-Heinemann, Oxford, UK*, 483.

Kubo, N., & Shimura, H. (1999). Theoretical analysis of transient phenomena of conveyance waves with small froude number. *Trans. Jpn. Soc. Irrig. Drainage Reclamation Eng.(In Japanese)*, *138*, 25-36.

Lighthill, M. J., & Whitham, G. B. (1955). On kinematic waves. i: Flood movement in long rivers. *Proc. R. Soc. London, Ser. A*, *229*, 281316.

Malaterre, P. O., & Baume, J. P. (1998). Modeling and regulation of irrigation canals: Existing applications and ongoing researches. *IEEE international conference on systems, man and cybernetics, San Diego, CA*, 3850-3855.

Nelz, S., & Pender, G. (2009). Desktop review of 2d hydraulic modelling packages. *En-*

vironment Agency, Rio House, Waterside Drive, Aztec West, Almondsbury, Bristol, BS32 4UD.

Odai, K., Onizuka, & Osato. (2006). Analytical solution of the burgers equation for simulating translatory waves in conveyance channels. *Journal of Hydraulic Engineering*, 194-199.

Odai, S. N. (1999). Nonlinear kinematic-wave model for predicting open-channel flow rate. *J. Hydraul. Eng*, *125*(8), 886889.

Onizuka, K., & Odai, S. N. (1998). Burgers equation model for unsteady flow in open channels. *J. Hydraul. Eng*, *124*(5), 509512.

P. Krause, D. B., & F., B. (2005). Comparison of different efficiency criteria for hydrological model assessment. *Advances in Geosciences*, *5*, 89-97.

Price, R. K. (1994). Flood routing models. computer modeling of freesurface and pressurized flows, m. h. chaudhry and l. w. mays, eds. *Kluwer Academic Publishers, Dordrecht, The Netherlands*, 375-407.

Sleigh, P. A., & Goodwill, I. M. (2000). The saint venant equations.

Su Ki Ooi, E. W., M.P.M Krutzen. (2005). On physical and data driven modeling of irrigation channels. *Control Eng. Practice*, 461-471.

Szymkiewicz, R. (2010). Numerical modeling in open channel hydraulics numerical integration of the saint venant equations faculty of civil and environmental engineering. *Gda sk University of Technology*, 310-375.

Tsai, C. W. S. (2003). Applicability of kinematic, noninertia, and quasisteady dynamic

wave models to unsteady flow routing. *Journal of Hydraulic Engineering*, *129(8)*, 613-627.

Whitham, G. B. (1974). Linear and nonlinear waves. *Wiley, New York*, 45-50.

Yabe, T., & Aoki, T. (1991). A universal solver for hyperbolic equations by cubic-interpolation. i. one-dimensional solver. *Comput. Phys. Commun.*, *66*, 219232.